Site-specific rock-fall parameters in a hard rock open pit environment.

Jacques du Toit

Student number: 713279

School of Mining Engineering

University of the Witwatersrand

Johannesburg, South Africa.

Supervisor:

Prof T.R. Stacey

A research report submitted to the Faculty of Engineering and the Built Environment, University of the Witwatersrand, in fulfilment of the requirements for the degree of Master of Science in Engineering.

Date:

2015/09/11

Declaration

I declare that this research report is my own, unaided work. It is being submitted for the degree of Master of Science in Engineering to the University of the Witwatersrand, Johannesburg. It has not been submitted before for any degree or examination in any other University.

Student:

day of (year)

signed at the University of the Witwatersrand, Johannesburg.

Abstract

This research report is focussed on rock-fall in an open pit mine. Rock-fall is a well-known hazard in open pit mining, housing, and railway and road cuttings. The prediction of accurate rock-fall trajectories is vitally important to ensure the safe construction and operation of these projects. All current rock-fall software uses stereomechanical impact theory, which assigns Normal and Tangential Coefficients of Restitution (CoR) to a collision where permanent deformation is experienced. The Kinematic CoR describes the amount of energy lost as a ratio between energy before and after impact. The Tangential CoR and Normal CoR are vector components of the Kinematic CoR.

Rock-fall modelling is reliant on the specification of a representative Coefficient of Restitution to enable the determination of accurate rock-fall trajectories. This is currently done by adding statistical variation to the CoR to establish different possible rock-fall trajectories. The output is used in rock-fall barrier or geotechnical catch berm design for slopes. Different ways to establish the most applicable CoR for rock-fall modelling were studied through in-situ testing, with associated calculations, software calibration, and laboratory testing. From the in-situ testing, three correlations were found to estimate the trajectories of rock blocks with good accuracy.

A negative exponential correlation was found between the impact energy and Kinematic CoR, known as "ESCORSE", the **E**nergy **S**pecific **CoR** **S**election **E**nvelope. Two separate linear correlations between the Kinematic CoR and Tangential CoR, and, Kinematic CoR and Normal CoR were determined. The influence that this research will have on rock-fall simulations is that the selection of a CoR is not only dependent on the rock type, but also on the energy conditions at impact - once the rock has passed the elastic impact boundary, the greater the impact energy the greater the energy loss due to fracturing.

Further study is needed to define the ESCORSE for softer and harder rock types, including the linear relationships between the Kinematic CoR and Tangential CoR, and, the Kinematic CoR and Normal CoR.

Acknowledgements

I would like to express my gratitude to The University of Witwatersrand for the opportunity to add all the experience to my professional skillset and to Professor T R Stacey for the guidance throughout my studies.

Anglo American Platinum is thanked for financial assistance.

Contents

List of Equations

List of Figures

List of Tables

List of Symbols

Chapter 1

Introduction

Rock falls from the slopes of road and rail cuttings, natural cliffs and open pit mine slopes can be a major hazard to the safety of the public and mine personnel. In addition, disruption due to such falls can have a significant economic impact. Research into rock-fall behaviour is therefore important. The prediction of rock-fall trajectories and run out distances is usually carried out using available software packages. At Mogalakwena open pit mine it has been found that there is a poor correlation between these rock-fall predictions and the observed behaviour. This appears to be due to the breaking up of the rock boulders at impacts during their trajectories, with consequent loss of energy. These observations are the basis for this research project, which is focused on rock-fall and defining the amount of energy loss throughout the trajectory path due to impact. This will enable more accurate calculation of the rock-fall trajectory path. The data used in the report was gathered from Mogalakwena Platinum Mine.

Mogalakwena mine is owned by Anglo American Platinum. Shown in figure 1-1, is a geographical location map of the mine. The operational and planned pit positions consisting of Mogalakwena North-, Mogalakwena Central-, Mogalakwena South-, Zwartfontein South-, Sandsloot-, Tweefontein North- and Tweefontein Hill Pits, are shown in figure 1-2, on a mine scale map. The mine is situated 35km north of the town of Mokopane, in the Limpopo Province of South-Africa. Geologically, it is located in the well-known Bushveld Igneous Complex. The Bushveld Igneous Complex (Rustenburg Layered Suite) consists of the eastern, western and northern limbs of a mafic layered intrusion of a saucer-shaped nature, (Cawthorn, Walraven, Uken, & Watkeys, 2006). The mine is within the Bushveld Igneous Complex's northern limb. The targeted reef actively mined is the so-called Platreef, which has a general thickness of 100m. The reef strikes north to south, creating a tabular orebody dipping at 45 degrees to the west, reaching a depth of 2000m. The Platreef orebody hosts economic quantities of platinum, palladium, rhodium, gold, copper and nickel (Little, 2006).

As indicated above, rock-falls are a common hazard in open pit mines, quarries, mountainous areas, and road and railway cuttings. In mining this hazard is managed through a Mandatory Code of Practice which is enforced through the Department of Mineral Resources. In this report, rock-fall occurrence and prediction at Mogalakwena Mine will be discussed after giving a brief description of the geological conditions at the mine.

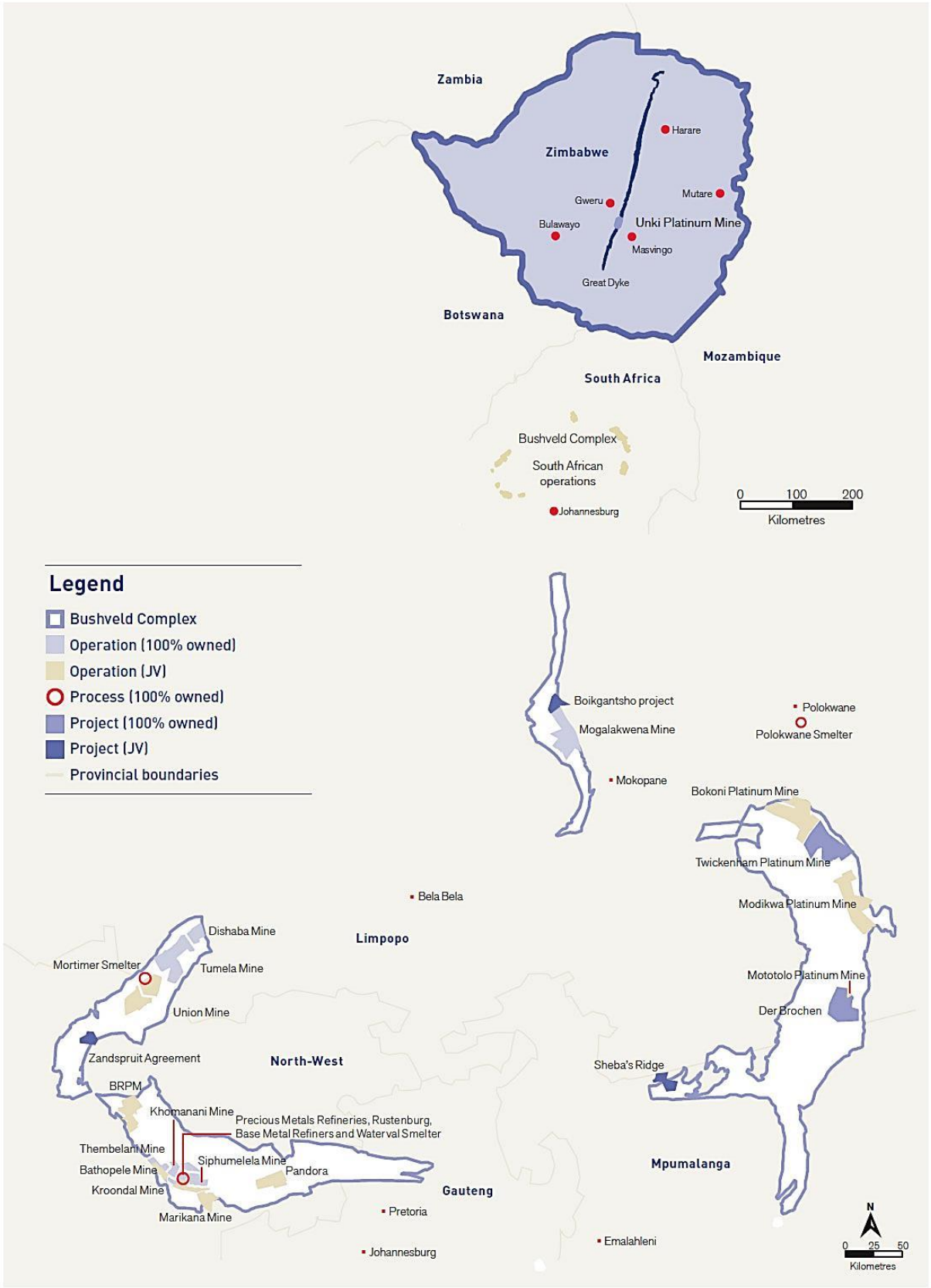

Figure 1-1: Location map of the outcrop of the Bushveld complex and the Anglo Platinum operations in 2013 (Anglo American Platinum, 2014)

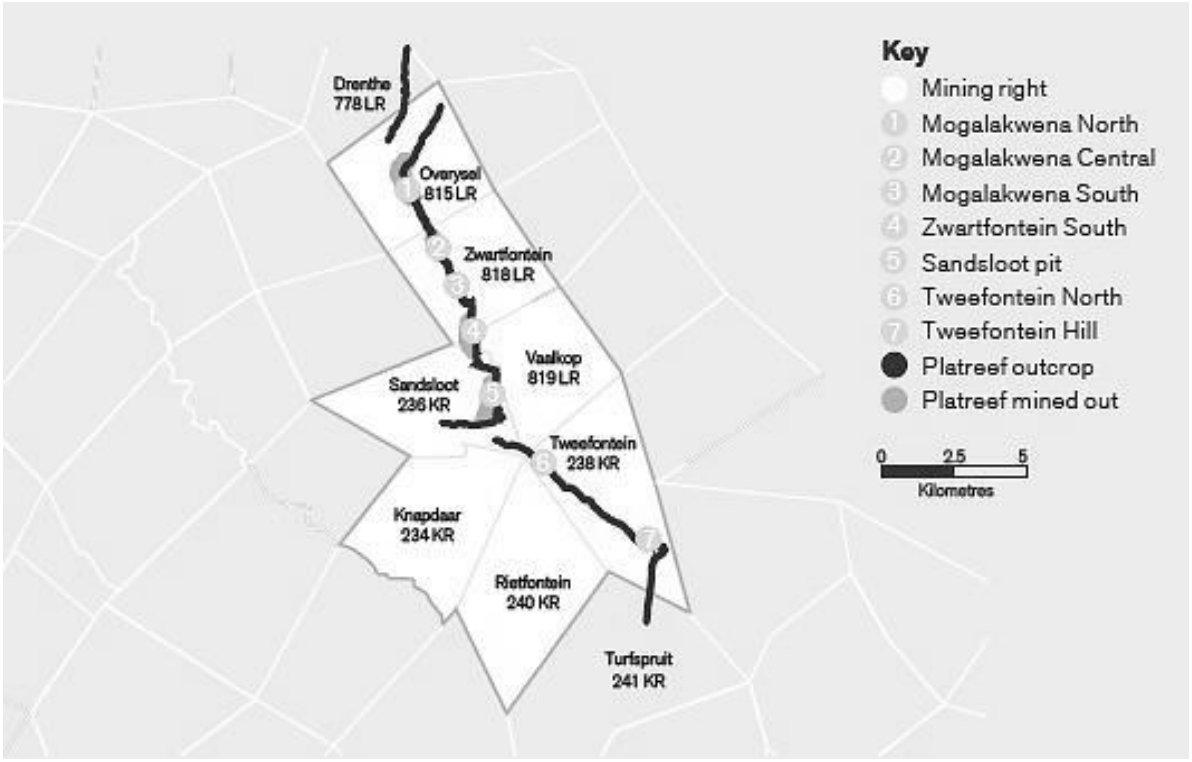

Figure 1-2: Shown are the five operational pits 1-5 and two planned pits 6-7 of Mogalakwena mine (Anglo American Platinum, 2014).

1.1. Stratigraphy

The Rustenburg Layered Suite consists of, from top to bottom, Upper, Main, Critical, Lower and Marginal Zones. In the northern limb, in which mining at Mogalakwena takes place, the older Marginal Zone is absent and the poorly developed Lower and Critical Zones only appear south of Mokopane. The northern-limb is mostly overlain by younger Waterberg Group sediments (Little, 2006).

The mining area is located where the platreef outcrops on surface. The stratigraphy from the northern extent of the mining property to the south is as follows (figure 1-3):

- Norite is the overlying rock type, with zero thickness at the Platreef outcrop, increasing in thickness to the west.
- The Platreef is at the bottom of the Main Zone, subdivided into three portions, C-reef, B-reef and A-reef from top to bottom. C-reef is a medium grained feldspathic pyroxenite, B-reef a coarse grained pyroxenite (showing the highest grades), and A-reef is a pegmatoidal feldspathic pyroxenite.
- At Mogalakwena North, Central and South, the footwall rock type is Archean granite with a metamorphic product granofels, forming between the Platreef and Archean Granite.
- At Zwartfontein and Sandsloot the footwall is Malmani dolomite, with the metamorphic product calc-silicate.

- At the most southern boundary, Tweefontein, the footwall consists of banded iron formation and shale, forming a hornfels metamorphic product between the platreef, banded iron formation and shale (Little, 2006).

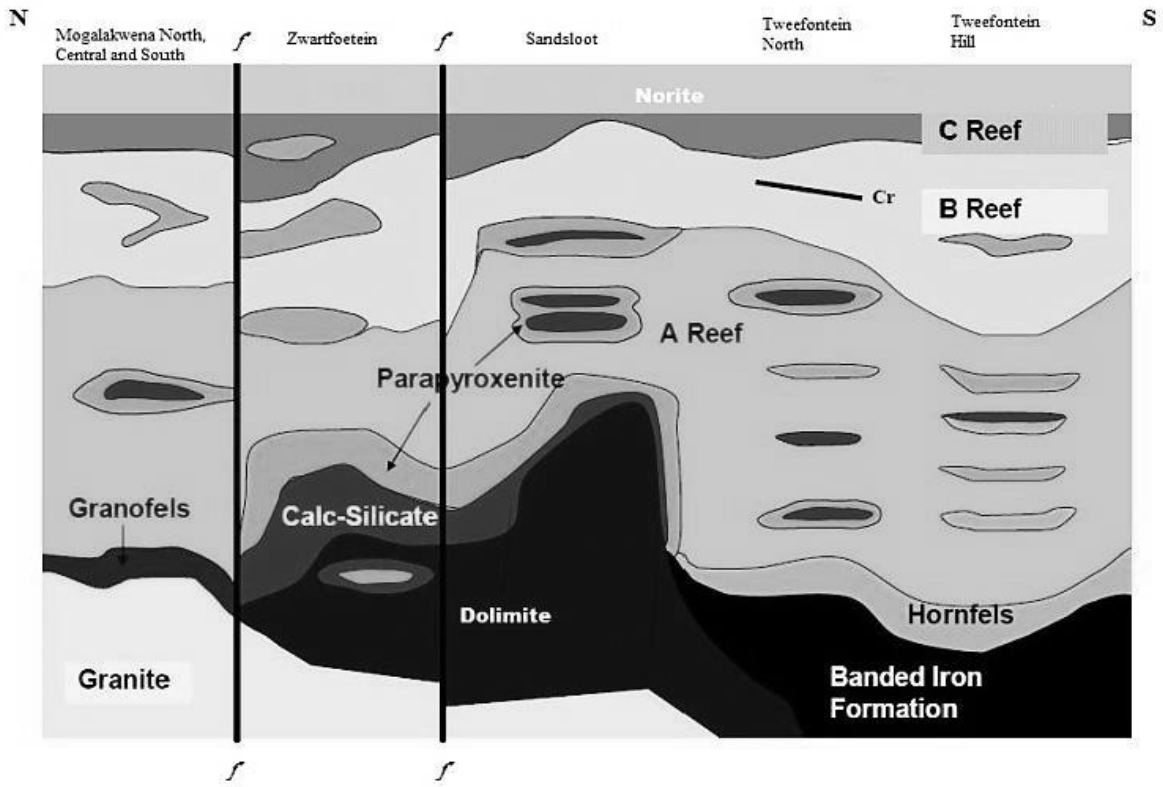

Figure 1-3: The cross section through the Platreef shows Mogalakwena Mine Pits from North to South with the different rock types at each (Little, 2006).

1.2. Open pit Mining

Mogalakwena Mine is a highly mechanised operation with the mining method being open pit mining. In open pit mining the design and management of slopes are the major challenges during the planning and operation of the mine.

There are various factors affecting the design of slopes, namely:

- Geological setting, in-situ stress, weathering, geological alteration, jointing, faulting, rock strength, joint strength and groundwater.
- Human controlled factors such as the excavation or blasting method (Read & Stacey, 2008).
- As part of the design process, the mode of potential failure that is taken into account - circular, toppling, planar, wedge or combinations thereof (Richards, 1992).

One of the major factors obstructing the safe operation of an open pit mine is rock-fall. Rock-fall is part of a slope's natural progression to equilibrium. This involves detachment of rock fragments, their trajectory, impact, subsequent rolling, sliding, bouncing and deposition at the foot of the slope

or on spill berms down the slope (Evans & Hungr, 1989). The most intense occurrences of rock-fall are in periods of low temperature and high rainfall (Asteriou et al, 2012 and Hoek & Bray, 2005).

In order to plan measures and effectively mitigate this hazard, the slope design is examined through rock-fall analysis techniques. This is to evaluate the required berm size, since the main function of geotechnical spill berms is to arrest rock-fall, thus ensuring that the rest of the slope below is safe. The width of geotechnical spill berms is the critical factor affecting both the slope angle and the arresting of a rock-fall (Little, 2006). In figures 1-4 and 1-5 one such rock-fall analysis is shown. The accuracy of modelling programs for rock-fall analysis is dependent on the correct estimation of input parameters and the ability to calibrate the results with actual rock falls (Wyllie, 2014).

Commercially available software uses the Normal- and Tangential Coefficients of Restitution (CoR) in the modelling of the rock-fall trajectory; the values are either assumed from empirical information or calibrated from in-situ tests.

Owing to the different ore body geometries, Mogalakwena Mine has different bench heights for the different pits, to better extract the ore:

- Mogalakwena North, Central and South have, from surface, a 10m bench height and 10m berm width to bench eight (1090-1080m above mean sea level); below there is a 3 bench stack geometry with 15m bench height and 10m berm width, with the following bench having a 20m geotechnical spill berm width.
- Zwartfontein pit has two slope configurations - a single and double bench as shown in figures 1-4 and 1-5. The single bench consists of a 10m bench height and 5m step-off berm width, followed by a 10m bench height and 10m berm width, figure 1-4. The double bench design comprises two 10m benches of the first configuration i.e. the bench height is 20m, with a 15m geotechnical spill berm width, figure 1-5.
- Sandsloot pit had various slope configurations; the final design was representative of the Mogalakwena pits design.
- Tweefontein designs are not yet finalized and therefore not described here.

The correct design of slopes is the first line of defence against major hazards such as rock-fall and slope failures. When the slope design is not achieved, the risk to personnel may become more than the acceptable levels and require the installation of artificial support, to reduce the risk. A common way of taking risk into account is to use modified rock-fall hazard rating systems (RHRS), as applied to highways (California Department of Transportation, 2014).

In the normal RHRS based on road works, the factors used to assess the risk are divided into failure causing factors, and consequences of failure. The risk due to rock-fall is highly dependent on the exposure of personnel and equipment to the hazard. With reference to natural slopes, it is well-known that the economic and social significance of large slope failures is dependent on the population density and infrastructure close to events. Failures of in excess of 2 square kilometres have gone unnoticed in unpopulated areas for many years (Hungr & Evans, 1993).

Some examples of failure causing factors within the RHRS are slope height, slope angle, rock face instability, degree of weathering, strength of intact rock, face irregularities, rock mass looseness, block size, presence of water, freeze/thaw action, blasting vibrations, seismicity and joint

orientation. Consequences of failure considerations include berm/ditch width, berm/ditch shape, berm/ditch volume, road shoulder width, number of lanes, average daily traffic, expected rock fall quantity, kinetic energy and line of sight distance.

Remedial measures for the RHRS are chosen considering the rating, and the appropriate slope support is allocated to specific situations (Richards, 1992), (Hoek & Bray, Rock Slope Engineering. Civil and Mining., 2005), (Youssef & Maerz, 2010), (Hoek E. , 2006) and (Read & Stacey, 2008).

The Swiss Federal Guidelines (SFG) apply a different concept to arrive at a hazard rating. The SFG is based on zoning areas where particular restrictions are placed, for high, moderate and low risk zones. In high risk zones, development is forbidden. In moderate risk zones, regulated areas with protective measures are zoned. Low risk zones are defined as a changing domain, where restrictions may or may not be placed, with people at slight risk of injury. The SFG is based on the intensity, total kinetic energy, and return period between 30-300 years, of rock fall (Budetta, 2011).

SFG remedial measures for unstable slopes include categories subdivided into warning, protection and stabilisation, excavation, scaling, floodwater diversion, groundwater drainage, wall control blasting, rock reinforcement, barricading, catch walls, draped mesh, pinned mesh, catch fences, catch nets, visual inspections, patrols and demarcation (Richards, 1992).

For open pit mining, these types of systems are modified and applied to remediate areas where geological conditions are adverse or mining did not achieve the designed slope. The success of an open pit mine will largely depend on the open pit design implemented and the management of any problems that develop during the operating life. Optimising the pit slope is a major factor on which profitability will depend. Good design, mining and monitoring will ensure safe and economical operation.

1.3 Structure of this research report

In the following Chapter, Chapter 2, a review of relevant literature dealing with rock-fall and the modelling of such events is presented. Chapter 3 deals with field tests carried out to provide data for calibration of prediction models. Model calibration based on the field testing is described in Chapter 4. In Chapter 5 the results of laboratory tests are presented, allowing “alternative” calculation of coefficient of restitution values for different rock types. These values would have been applied in discrete element modelling however funding was not available to obtain such software. In Chapter 6, the site specific rock-fall model is explained and presented. Conclusions from the research are presented in Chapter 7.

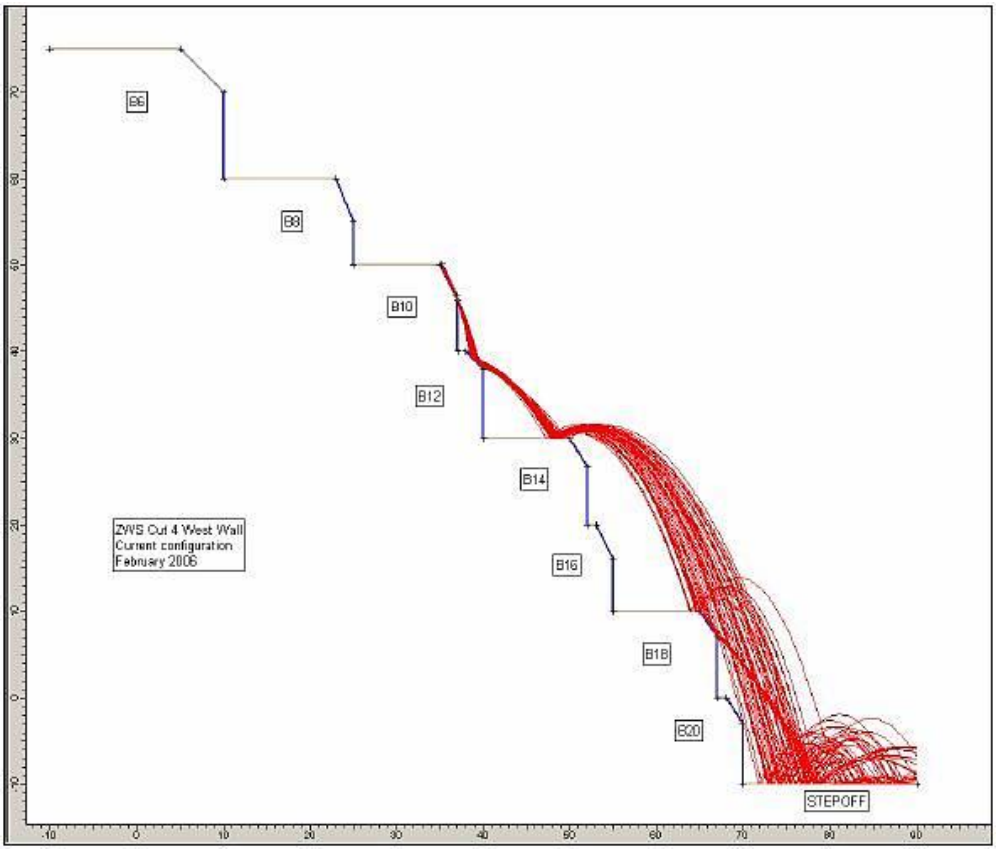

Figure 1-4: The single bench configuration of Zwartfontein pit, with a RocFall™ simulation (Little, 2006).

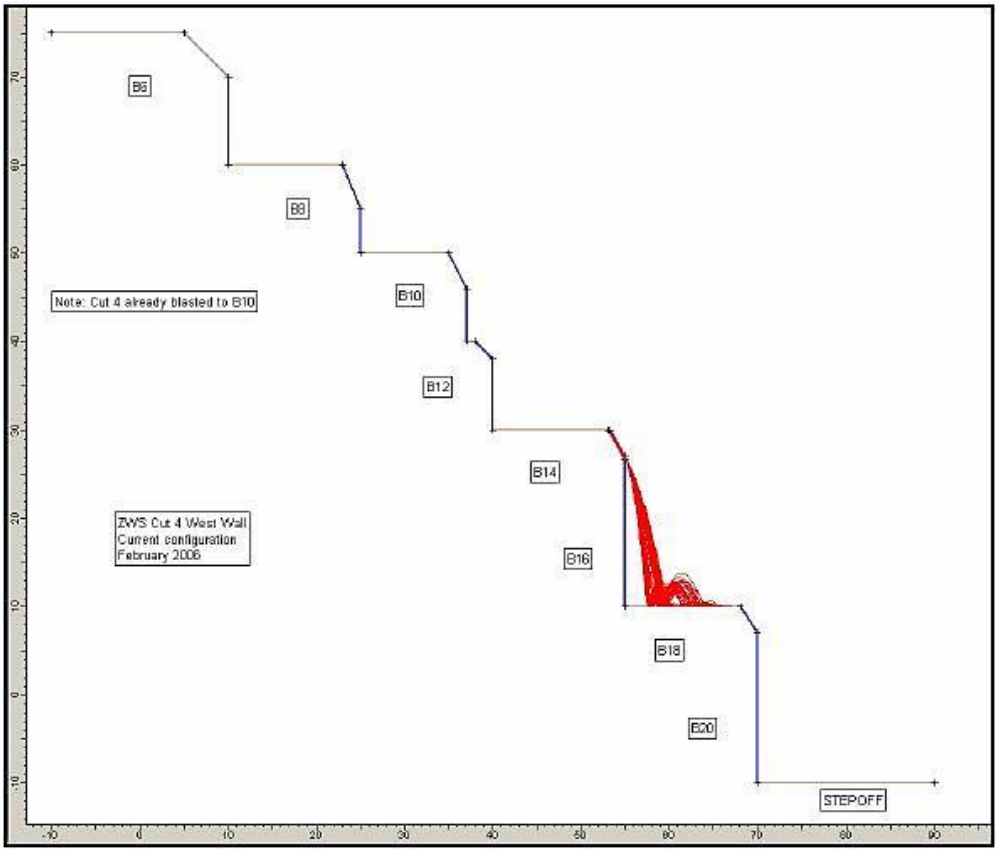

Figure 1-5: The double bench configuration of Zwartfontein pit, showing a RocFall™ simulation (Little, 2006).

Chapter 2

Review of relevant rock-fall literature and current understanding

In the preceding chapter the location of the study area was discussed along with how mine design helps in the mitigation of rock-fall risk to working personnel. Chapter 2 describes the origin of rock-fall, influencing factors, different coefficients of restitution (CoR) and the way these coefficients are determined, and how they relate to one another.

2.1. Introduction

In mountainous areas rock-fall is a well-known hazard (Evans & Hungr, 1989), (Wyllie, 2014), (Wang, et al., 2007), (Fornaro, Peila, & Nebbia, 1990), (Chau, Wong, & Wu, 2002), (Spadari, Giacomini, Buzzi, Fityus, & Giani, 2012) , (Asteriou, Saroglou, & Tsiambaos, 2012), (Giacomini, Buzzi, Renard, & Giani, 2009), (Guzzetti, Crosta, Detti, & Agliardi, 2002), (Hoek & Bray, Rock Slope Engineering. Civil and Mining., 2005) and (Hoek E. , 2006) . In the open pit mining environment rock-fall is also common. Rock-fall consists of two distinct phases, initial failure of the rock mass and the subsequent motion of a detached rock block down a slope (Asteriou, Saroglou, & Tsiambaos, 2012) and (Wang, et al., 2007). In this research only the latter was considered. The trajectory of a rock-fall is controlled by the source location, the boulder shape, the boulder geometry, the slope topography geometry and the material type (Guzzetti, Crosta, Detti, & Agliardi, 2002). There are four basic block movements which are, free fall, bouncing, rolling and sliding, (Basson, 2012), (Wang, et al., 2007), (Hoek & Bray, Rock Slope Engineering. Civil and Mining., 2005) and (Spadari, Giacomini, Buzzi, Fityus, & Giani, 2012). The CoR is the most critical input for predicting the extent of bouncing of a rock block (Asteriou, Saroglou, & Tsiambaos, 2012) and (Chau, Wong, & Wu, 2002). From the point of release the potential energy possessed by the block will transform into kinetic energy. As the rock block loses energy it will come to a stop once sufficient energy is lost. Energy loss due to air drag is mostly ignored (Guzzetti, Crosta, Detti, & Agliardi, 2002).

Rock structure, the degree of weathering and environmental and human induced factors such as erosion, saturation, freezing, undermining due to water runoff or mining, seismicity, plant roots, rainfall, thermal expansion and contraction cycles and blasting all affect rock-fall occurrence (Evans & Hungr, 1989), (Wyllie, 2014), (Giacomini, Thoeni, Lambert, Booth, & Sloan, 2012), (Asteriou, Saroglou, & Tsiambaos, 2012), (Read & Stacey, 2008), (Hoek & Bray, Rock Slope Engineering. Civil and Mining., 2005) and (Hoek E. , 2006). Both the frictional and restitution coefficients will be affected by various impediments encountered on a slope (Fornaro, Peila, & Nebbia, 1990).

All open pit operations attempt to mitigate the rock-fall hazard through adequate pit design, good blasting practices and removal of loose rocks through mechanical means (Giacomini, Thoeni, Lambert, Booth, & Sloan, 2012), (Hoek & Bray, Rock Slope Engineering. Civil and Mining., 2005), (Read & Stacey, 2008), (Little, 2006) and (Hoek E. , 2006). Open pit design caters for sufficient catchment, in the form of catch berms, in the event of structural failure or rock-fall. When the design is not achieved, other measures need to be considered to reduce the risk (Giacomini, Thoeni, Lambert, Booth, & Sloan, 2012), (Hoek & Bray, Rock Slope Engineering. Civil and Mining., 2005), (Hoek E. , 2006) and (Read & Stacey, 2008). Rock-fall protection systems are chosen and designed

according to possible rock block trajectories, which are usually modelled using commercially available software (Giacomini, Thoeni, Lambert, Booth, & Sloan, 2012) and (Giani, Giacomini, Migliazza, & Segalini, 2004).

Research regarding the mitigation of the hazard has mainly been focused on in-situ rock-fall, barrier tests, and the development of analytical and numerical models. These models are able to consider the trajectories of blocks under different morphological and geological conditions (Giacomini, Thoeni, Lambert, Booth, & Sloan, 2012), (Wang, et al., 2007), (Chau, Wong, & Wu, 2002), (Rocscience, 2003), (Asteriou, Saroglou, & Tsiambaos, 2012), (Spadari, Giacomini, Buzzi, Fityus, & Giani, 2012)and (Hoek E. , 2006). The effect of an impact point load, and small stress concentrations at the point of impact, has not been well studied, nor the effect that this has on the fragmentation of the falling boulder after impact. The difference between the trajectories of the smaller fragments, as well as their possessing higher velocities, and the trajectory of the original boulder is neglected in current commercial software (Wang & Tonon, 2011) and (Giacomini, Buzzi, Renard, & Giani, 2009). When any inelastic or permanent deformation takes place on impact or collision, a CoR, based on stereomechanical impact theory must be considered (Asteriou, Saroglou, & Tsiambaos, 2012), (Chau, Wong, & Wu, 2002) and (Goldsmith, 2001). The CoR may describe different types of behaviour namely, elastic, inelastic or plastic. A purely elastic collision will have a CoR equal to one. This is illustrated in figure 2-1. An inelastic collision's CoR will range from one to zero and a pure plastic collision will be equal to zero (Goldsmith, 2001), (Asteriou, Saroglou, & Tsiambaos, 2012). The elastic to plastic behaviour of a rock block is dependent on the impact angle, boulder mass, velocity and mechanical properties of the slope and boulder material (Wang & Tonon, 2011), (Guzzetti, Crosta, Detti, & Agliardi, 2002).

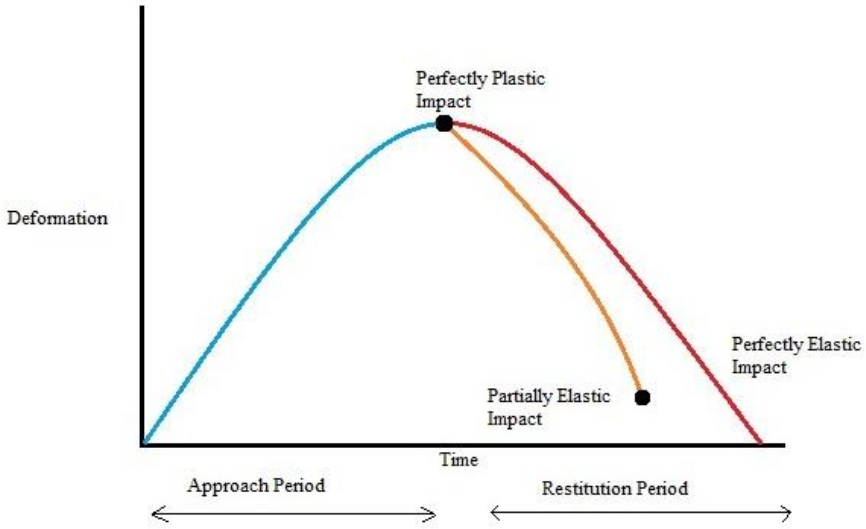

Figure 2-1: A purely plastic impact deforms to a maximum and has no rebound (restitution); an impact with some permanent deformation will be a Partially Elastic, and a fully elastic impact will recover all deformation (Goldsmith, 2001).

There are three possible alternatives in the derivation of the CoR namely, kinematic, kinetic and energy approaches. The most commonly used approach, due to its simplicity of application, is the

kinematic CoR derived from the lumped-mass or Stereomechanical impact theory (Chau, Wong, & Wu, 2002), (Asteriou, Saroglou, & Tsiambaos, 2012).

From laboratory tests it is observed that even in the elastic region some energy is dissipated, due to the effect of hysteresis on a test sample. Hysteresis is embodied by a loop in the stress/strain curve during consecutive loading and unloading cycles (Asteriou, Saroglou, & Tsiambaos, 2012). What this is showing is that mineral grains do not recover immediately to their original shape. This hysteretic damping ratio of the unloading energy to the loading energy can be quantified as the CoR (Imre, Rabsamen, & Springman, 2008). This property will be considered in investigating the possibility of using laboratory CoR values as input data for rock fall simulations.

2.2. Kinematic coefficient of restitution

The kinematic CoR can either be calculated by height or velocity (Asteriou, Saroglou, & Tsiambaos, 2012).

Kinematic CoR (v_{CoR}) calculated by height:

$$\boldsymbol{v_{CoR}} = \sqrt{\frac{\boldsymbol{hr}}{\boldsymbol{hd}}} \qquad \textbf{Equation 1}$$

Where h_r is the rebound height and h_d is the release height of the rock block, (Richards, 1992), (Basson, 2012) and (Asteriou, Saroglou, & Tsiambaos, 2012).

Kinematic CoR (R_v) calculated by velocity:

$$\boldsymbol{R_v} = \frac{\boldsymbol{v_r}}{\boldsymbol{v_i}} \qquad \textbf{Equation 2}$$

Where v_r is the rebound velocity and v_i is the impact velocity of the rock block (Giacomini, Thoeni, Lambert, Booth, & Sloan, 2012), (Spadari, Giacomini, Buzzi, Fityus, & Giani, 2012), (Asteriou, Saroglou, & Tsiambaos, 2012), (Wang, et al., 2007)and (Chau, Wong, & Wu, 2002).

This equation can be expressed in normal (R_n) and tangential (R_t) components.

Normal CoR (R_n) is calculated by:

$$\boldsymbol{R_n} = \frac{\boldsymbol{v_{nr}}}{\boldsymbol{v_{ni}}} \qquad \textbf{Equation 3}$$

Where v_{nr} is the normal rebound velocity and v_{ni} is the normal impact velocity of the rock block (Wyllie, 2014), (Giacomini, Thoeni, Lambert, Booth, & Sloan, 2012), (Spadari, Giacomini, Buzzi, Fityus, & Giani, 2012), (Basson, 2012) and (Asteriou, Saroglou, & Tsiambaos, 2012). The normal CoR is associated with energy dissipation due to the elasto-plastic response of the surface material (Spadari, Giacomini, Buzzi, Fityus, & Giani, 2012).

Tangential CoR (R_t) is calculated by:

$$\boldsymbol{R_t} = \frac{\boldsymbol{v_{tr}}}{\boldsymbol{v_{ti}}} \qquad \textbf{Equation 4}$$

Where v_{tr} is the tangential rebound velocity and v_{ti} is the tangential impact velocity of the rock block (Wyllie, 2014), (Asteriou, Saroglou, & Tsiambaos, 2012) and (Chau, Wong, & Wu, 2002). The

tangential CoR is associated with the frictional dissipation of energy and with the roughness of the impacting surface. The normal and tangential components used in equations 2, 3 and 4 are shown in figure 2-2.

An energy based CoR can also be calculated (Giacomini et al, 2009; Chau et al, 2002). The total kinetic energy consists of two components:

- Translational kinetic energy
- Rotational kinetic energy

The translational kinetic energy (E_v) is defined by:

$$\boldsymbol{E_v = \frac{1}{2}mv^2} \qquad \textbf{Equation 5}$$

Where *m* is the mass (kg) and *v* is the velocity (m/s), (Richards, 1992), (Giancoli, 2005) and (Giacomini, Thoeni, Lambert, Booth, & Sloan, 2012).

The rotational kinetic energy (E_r) is defined by:

$$\boldsymbol{E_r = \frac{1}{2}Iw^2} \qquad \textbf{Equation 6}$$

Where *I* is the moment of inertia around the rotation axis (kg.m^2) and *w* is the angular velocity (rad/s), (Giancoli, 2005) and (Giacomini, Thoeni, Lambert, Booth, & Sloan, 2012).

Energy CoR (R_E) is calculated by:

$$\boldsymbol{R_E = \sqrt{\frac{\frac{1}{2}mv_r^2}{\frac{1}{2}mv_i^2}} = \sqrt{\frac{v_r^2}{v_i^2}}} \qquad \textbf{Equation 7}$$

Where *m* is the mass of the boulder and v_r and v_i are the rebound and impact velocities respectively (Giacomini, Buzzi, Renard, & Giani, 2009) and (Chau, Wong, & Wu, 2002).

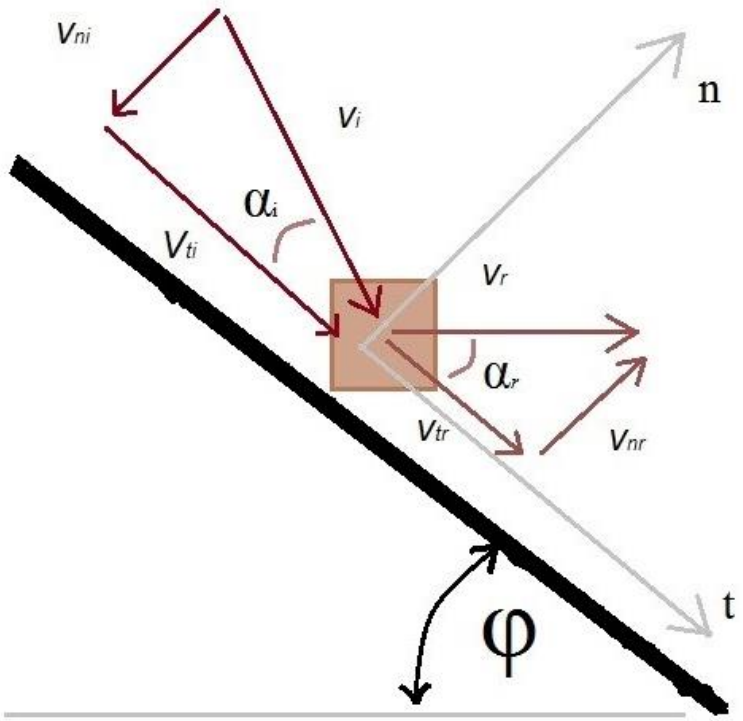

Figure 2-2: All velocity components of translational velocities before and after impact (Asteriou, Saroglou, & Tsiambaos, 2012).

2.3. Velocity scaling factor

Velocity scaling factor B gives an apparent relationship between the normal coefficient of restitution and impact velocity. Velocity scaling factor transitions the behaviour at low impact velocities from nearly elastic to inelastic conditions caused by fracturing of the rock and the impact surface at high impact velocities.

$$\boldsymbol{scaling\ factor\ (B)} = \frac{1}{1+(\frac{V_{ni}}{K_v})^2} \qquad \textbf{Equation 8}$$

Where v_{ni} is the normal impact velocity and K_v is an empirical constant 9.14m/s (Rocscience, 2003), equation 8.

The scaling factor is used to calculate a "scaled Normal CoR" to dampen the normal component of the CoR.

Rn (scaled) = Rn * scaling factor (B)

2.3.1. Fragmentation energy (EUR)

There have been various studies into proving and disproving the fragmentation energy threshold or EUR, by correlating the impact energy with fragmentation (Spadari, Giacomini, Buzzi, Fityus, & Giani, 2012). Using equation 9 the EUR may be calculated, and the EUR envelope is shown in figure 2-3.

$$\log(\boldsymbol{EUR}) = \boldsymbol{A} \times \boldsymbol{d}$$ **Equation 9**

Where A is an experimentally determined parameter using a rock hammer and d is the average block diameter (Fornaro, Peila, & Nebbia, 1990). This leads to the ability to calculate the energy that will be dissipated in an impact for a particular boulder size.

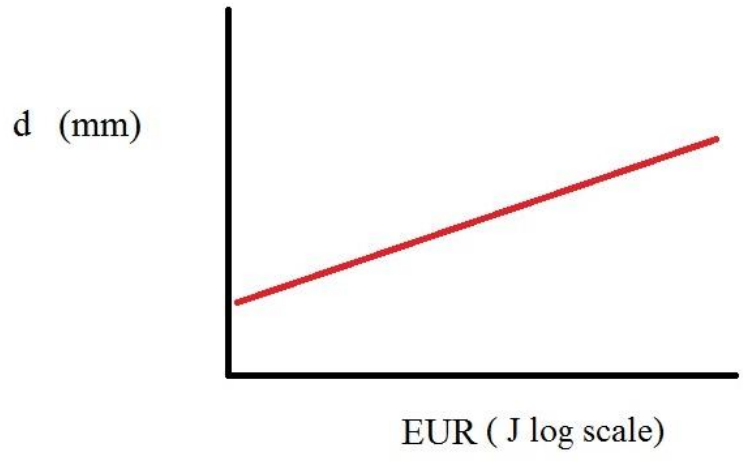

Figure 2-3: There the EUR envelope is shown that gives the energy of a particular size rock and the energy needed to fracture it (Fornaro, etal. 1990).

The EUR value depends on the rock type, shape and fractures within the block. Wang & Tonon, (2011) found, through discrete element modelling, that the factors affecting fragmentation are impact velocity, angle of incidence, pre-existing fractures and the impacting surface stiffness. Fragmentation size is very dependent on pre-existing fractures, without which there is only some fragmentation at the impact zone. Energy loss involves both friction and tensile crack generation, with only the first mentioned having a noticeable contribution. Wang & Tonon, (2011) also alluded to a threshold value for the impact normal stress at which fragmentation will occur, which is limited by the stiffness of the impacted ground.

Boulders impacting a surface at a large impact angle (90 degrees) will generate high impact stresses, increasing the chances of fragmenting blocks. Smaller impact angles (30 degrees) will reduce the chances of fragmenting blocks, but will increase the angular momentum of the impacting blocks (Wang & Tonon, 2011).

Giacomini et al, (2009), reported a constant amount of energy used to break (fragment) boulders. However, no correlation between the amount of fragments and the amount of energy was obtained. A correlation between the normal CoR and the amount of impact energy used in breaking was obtained: for an R_n = 0.6 amount of 10% impact energy was used and for an R_n = 0.8 an amount of 60% of the impact energy was used to break (fragment) the boulders.

It could be expected that the fragmentation energy should be an obtainable factor since the same phenomena are present in blasting engineering: to increase the fragmentation of rock, the Powder factor, weight of explosive or in other words the energy in the volume of rock is increased. Geological discontinuities do play a role in creating weakness planes through which energy is dissipated, thus decreasing the efficiency with which the explosive energy can achieve finer fragmentation.

2.4. Quasi-static energy coefficient of restitution

A rock sample can be deformed by two different modes of loading, either slow or fast: slow quasi-static loading will strain the entire specimen at a low strain rate; or an impulse that occurs over a short time period and only strains a small portion of a sample at a high strain rate (Imre et al., 2008). Uniaxial compressive strength (UCS) tests, carried out on rock specimens, correspond to the first mentioned, and the latter has greater similarity with conditions under impact.

In rock mechanics, the pre-yield section of a stress-strain curve is considered to be elastic. This means that all the deformation will be recovered when the sample is unloaded (Jager & Ryder, 2002). However, a sample will show some degree of hysteresis in the elastic region, due to elastic deformation stored by the sample during loading (Asteriou, Saroglou, & Tsiambaos, 2012). Consecutive loading and unloading cycles will result in hysteretic damping of the sample and this can be computed as the CoR, from triaxial compression tests, as shown in equation 10 (Imre, Rabsamen, & Springman, 2008).

$$\boldsymbol{CoR} = \frac{\boldsymbol{W_{UL}}}{\boldsymbol{W_L}} \qquad \textbf{Equation 10}$$

W_{UL} is the work done by triaxial unloading.

W_L is the work done by triaxial loading.

The work W done by the sample, calculated as the work done per unit cross-sectional area A, is expressed as:

$$\boldsymbol{W = Al \int (\sigma'_1 - \sigma'_3) d\varepsilon_1} \qquad \textbf{Equation 11}$$

l is the initial specimen length.

$(\sigma'_1 - \sigma'_3)$ is the deviatoric stress.

ε_1 is the axial strain.

This method of determining the quasi-static CoR includes the inaccuracies inherent in the compression test method, external friction from the loading platens, and the microscopic flaws in the test specimen. Nevertheless, in spite of these effects, according to Imre et al (2008), the method will still give an accurate determination of the CoR for site specific application.

2.5. Summary

Rock-fall studies have generally been focused on mountainous regions, as reflected in the literature, and consequently mining has adopted most systems for examining this hazard from these and civil road and railway applications.

The manner in which different coefficients of restitution are determined was also discussed. For practical use they are separated into normal and tangential vector components of the Kinematic CoR. There are also two concepts to down-scale the coefficients of restitution, namely the velocity scaling factor and fragmentation energy envelope (EUR).

In the following chapter the processing of the resulting data of field tests, will be described.

Chapter 3

Field Tests

In Chapter 2, relevant literature was reviewed to provide an understanding of rock-fall in an open pit context.

In order to calibrate a rock fall model, site specific data must be available. Such data can then be used for comparison with the output from computer software so as to ensure satisfactory calibration. Three rock-fall tests were conducted at Mogalakwena Mine, on the 8th and 28th of November and 5th of December 2011. All the tests were preceded by a risk assessment, and careful planning. Selected rock blocks were pushed over the crest of the slope by a backhoe to initiate the rock-fall motion. This induced both translational and rotational velocities. These tests are the basis of the information used to formulate the site specific rock-fall model.

3.1. Site Identification

A risk assessment relevant to the sites was carried out to plan for any unwanted event that may harm any of the participants or any other employees at Mogalakwena Mine. During the risk assessment, a task procedure was drawn up to inform all participants of their roles within the test.

On the Eastern Highwall (Figure 3-1), of Mogalakwena Central-Pit, the test sites were chosen where there was limited catchment, to ensure the rock-fall trajectory extended to the pit floor. Thus these sites were located where blast damage reduced geotechnical catchment (non-flat bench configurations).

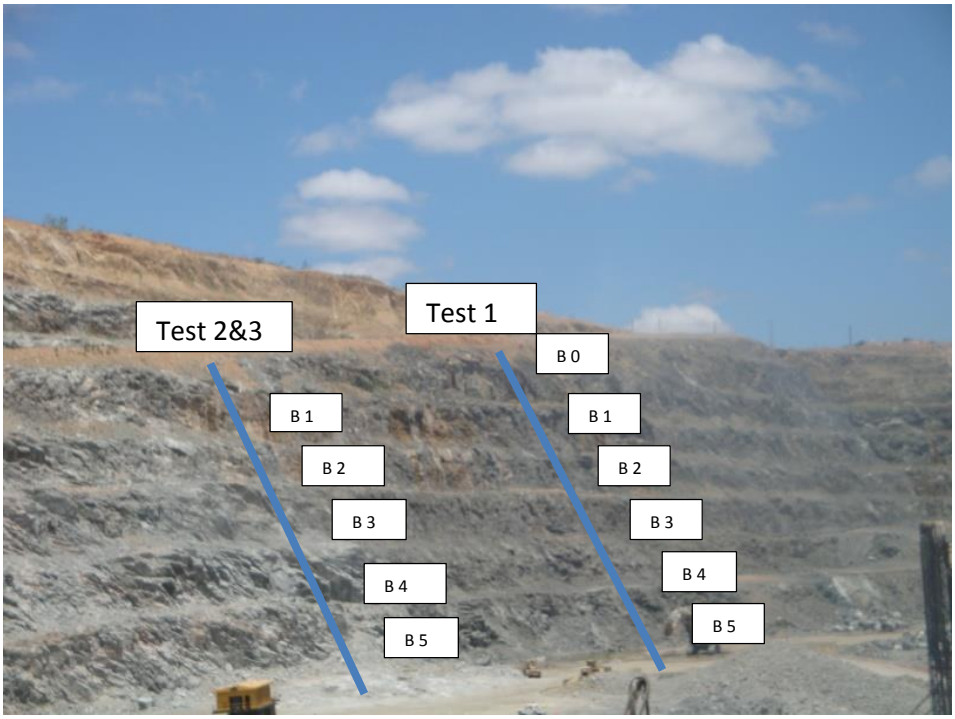

Figure 3-1: Test sites are located on the Eastern Highwall of Central pit.

3.2. Site Layout

The camera position chosen was perpendicular to the direction of travel of the rock-fall. This was to eliminate distortion due to the angle between the line of sight and direction of travel: with the chosen position (at right angles), the true height of the block could be taken into account. A high-speed camera was used to record the tests to ensure that the block would be located and traced. Thereafter the block velocities were calculated, before and after impact.

Positions were identified where the camera, mobile excavator and personnel guarding access to the test site were to be positioned (Figure 3-2). The ramp was closed above the Backhoe to prevent access to the pit bottom. Two guards were located to the left and right of the end position approximately 100 metres away. All personnel were in radio communication with each other and used the radio channel most frequently used on mine premises.

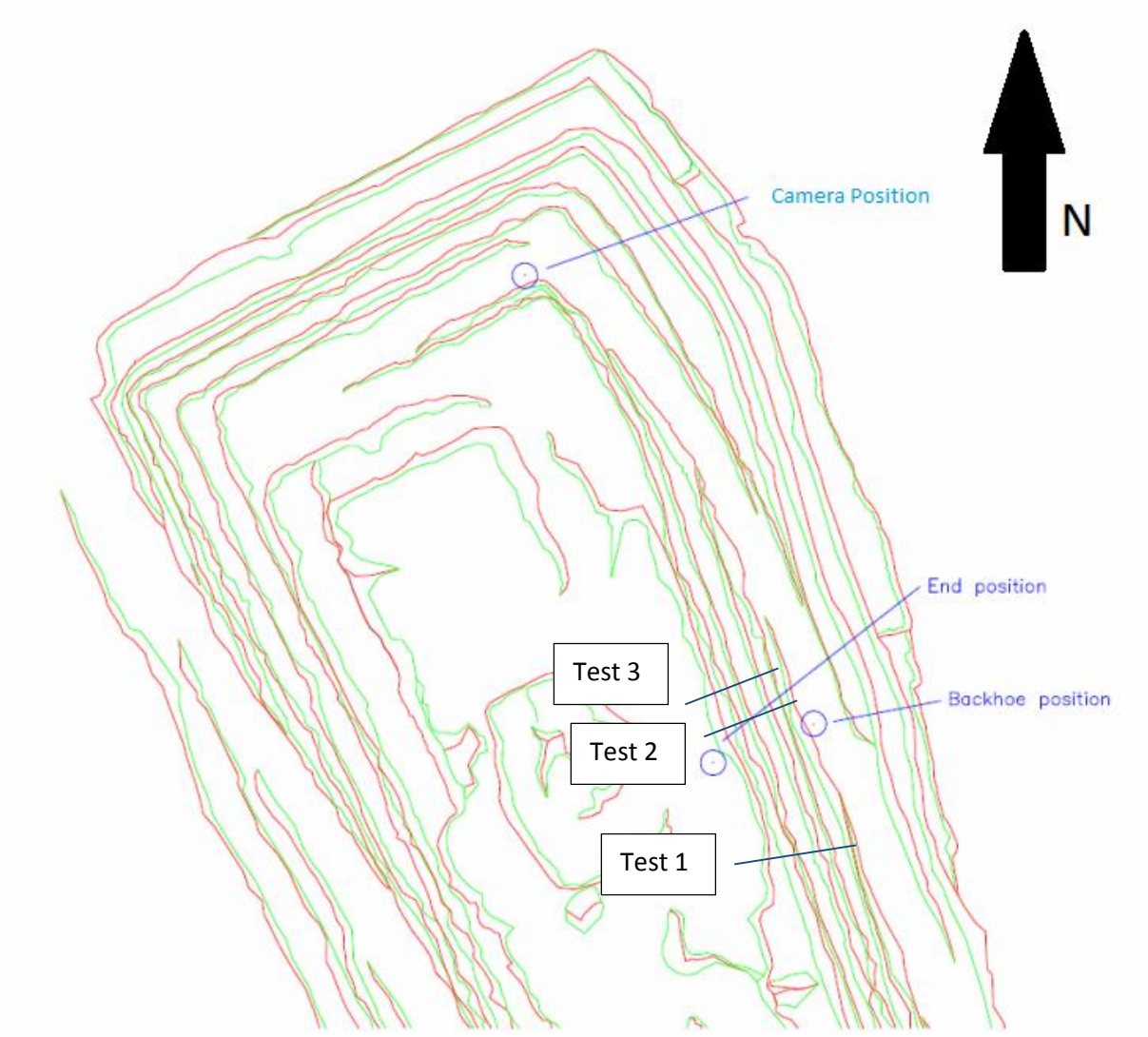

Figure 3-2: Positions of camera, backhoe, and end position of the rock blocks for Rock-fall test 2. Rock-fall test 1 was to the south and rock-fall test 3 to the north of the indicated position.

In the first test, both a high-speed camera used for blasting analysis and a Nikon D300s camera were used. It was found that the Nikon D300s was able to take sufficiently detailed images for the purpose of rock-fall profiling. The start of each run was counted down over radio communication to synchronize the releasing of the rock blocks and recording of the run.

3.3. Test Procedure

Block sizes are shown in table 3-1. The blocks were selected from muck piles (Figure 3-3) located underneath the Eastern Highwall, in an attempt to use rock material that would be representative of the in-situ material properties and size (block size caused by jointing).

Table 3-1: Rock-fall test number, with the block volume per run.

Rock-fall test	Run	Approximate Volume (m^3)	Block Mass (kg)
1	1	0.08	230
	2	0.08	230
	3	0.25	719
	4	0.11	316
2	1	0.208	598
	2	0.08	230
	3	0.252	725
3	1	0.208	598
	2	0.08	230
	3	0.252	725

Figure 3-3: A muck pile showing one of the blocks selected for rock-fall testing.

All materials were placed into position before the commencement of the tests. The personnel and equipment then moved into position. The access was then closed before the commencement of the tests. The reopening of the access was done after the area was declared safe by observers at the bottom of the pit after each test.

3.4. Test Results

The blocks were pushed into motion over the crest by a backhoe. This induced both translational and rotational velocities. The images from each of the test runs were printed and traced to paper,

Appendix 1, Test 1 was omitted due to the blocks being stopped on catchment berm B 3 from the pit crest. A cross section of the pit Highwall was taken and the misalignment of the camera position was corrected by taking the section at the same angle as the distortion. Relevant information was obtained from the rock-fall runs such as Kinematic CoR, Normal CoR, Tangential CoR, impact angle, rebound angle, impact angle from horizontal, slope angle, Mass (kg), Velocity, Impact Energy (kJ), Impact at bench (from the top down) and block diameter (m).

All the kinematic, normal and tangential coefficients of restitution are summarised in table 3-2. The calculated velocities were determined using the two nearest measurements for both impact and rebound trajectories.

3.4.1. In-situ test 1

The first test showed that the rock blocks were stopped by debris on the first geotechnical catchment berm or B 3 from the pit crest. Thus these Rock-fall trajectories were not traced. At the position of in-situ test 2 and 3 the geotechnical catchment was reduced due to blast damage. This enabled the rock-fall to progress to pit bottom.

3.4.2. In-situ test 2 and 3

The data from this test show the trajectories in cross-section in **Appendix 1**. At various impacts during the event, small fragments broke from the boulders at the impact area. These fragments then travelled at a much higher velocity and a different trajectory than the parent boulder. This can be due to the smaller mass of the fragments coupled with the fact that they originate from a small area with a high local stress concentration, i.e. small volume with a high energy concentration, imparting high energy on a small fragment. The smaller fragments were not able to be traced due to their size and colour, they faded into the back ground. Some of the larger fragments were traced and after an initial acceleration due to the impact behaved similarly to the host block.

From the results of the in-situ tests it is evident that in-situ testing is not an ideal way to determine the kinematic, normal and tangential coefficients of restitution. There are various problems associated with this procedure: the clarity and visibility of the projectile are not ideal; rotational components cannot be calculated; the type of impacting material cannot be precisely determined in all cases; and, finally, the impact and rebound angles are assumed from the angle of the slope, which is not precise.

There is no official standard practice or suggested method to determine rock-fall parameters from in-situ testing.

Table 3-2: Kinematic, normal and tangential coefficients of restitution from rock-fall tests 2 and 3.

Rock-fall test	Run	Impact	R_v	R_n	R_t	α_i	α_r	φ	Impact angle from horizontal	Mass (kg)	Velocity (m/s)	Impact Energy kJ	Impact at bench (down)	d (m)
2	1	1	0.75	1.06	0.61	30°	45°	48°	78°	598	13.13	51.5	5	0.62
	2	1	0.56	0.43	0.57	18°	14°	40°	58°	230	19.7	44.6	4	0.44
	3	1	0.47	0.94	0.32	23°	51°	39°	62°	725	18.6	125.4	3	0.67
	Average		0.59	0.81	0.5	23.67°	36.67°	42.33°	66°					
	Standard deviation		0.14	0.33	0.16	6.03°	19.86°	4.93°	10.6°					
3	1	1	0.5	0.84	0.39	24°	43°	42°	66°	598	21.88	143.1	5	0.62
	2	1	0.75	1.29	0.67	18°	32°	52°	70°	230	17.51	35.3	2	0.44
		2	0.56	0.76	0.53	19°	26°	37°	56°	230	17.51	35.3	3	0.44
		3	0.38	0.54	0.34	21°	31°	45°	66°	230	17.51	35.3	4	0.44
	3	1	0.5	0.79	0.37	29°	50°	48°	77°	725	19.375	136.1	2	0.67
		2	0.38	0.63	0.35	14°	24°	46°	60°	725	17.51	111.1	3	0.67
		3	0.45	0.58	0.41	27°	36°	46°	73°	725	21.88	173.5	5	0.67
	Average		0.5	0.78	0.44	21.71°	34.57°	45.14°	66.9°					
	Standard deviation		0.13	0.25	0.12	5.28°	9.27°	4.71°	7.3°					

(Refer to section 2.2.2 and figure 2-2 for clarity on symbols)

3.4.3. Interpretation

Correlations between the CoR and various parameters influencing the trajectory were investigated.

The tangential and normal coefficients of restitution were plotted against one another to determine whether any trends could be observed (figure 3-4). It was observed that heavier boulders generally have smaller tangential coefficients of restitution than the lighter boulders. The normal coefficients of restitution vary considerably for light boulders, but are more consistent for the heavier boulders.

This appears to indicate that the frictional component of the slope material has less of an influence on the tangential coefficient of restitution, and that the impact energy dissipation of the surface has a larger influence on the normal coefficient of restitution. Thus the latter has a greater influence on the rock-fall trajectory.

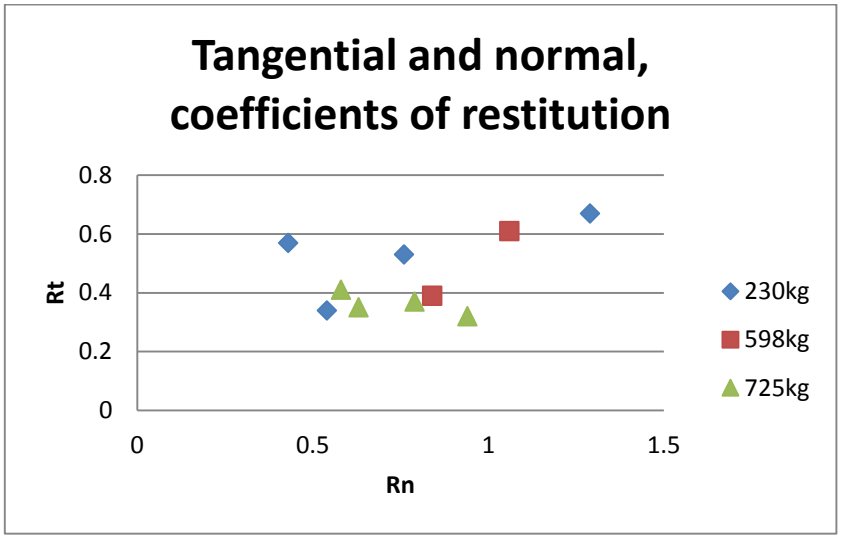

Figure 3-4: The Tangential and normal coefficients of restitution; in different colours are the different masses of boulders

Impact angle and impact location along the slope are plotted against CoR in figure 3-5, but there are no clear trends visible. It can be seen that heavier boulders impacted at higher angles. Figure 3-6, tangential CoR, with low values compared to the normal CoR, imply a larger reduction in tangential velocity. The normal coefficients of restitution were larger than expected and the tangential coefficients of restitutions lower, figure 3-6, not as reported by Guzzetti et al, (2002), who indicated the contrary.

The kinematic CoR, in figure 3-7, shows that lighter blocks are deflected and heavier blocks are slowed much more, even at low impact angles. These results indicate that the larger blocks are slowed more than the lighter blocks, and that the lighter blocks are deflected more at the same impact angles.

The impact velocity plotted against the location down the slope showed that the velocity is relatively constant, with only slight increases on two occasions, figure 3-8. No increase in impact velocity lower down the slope was observed. No satisfactory correlations were observed.

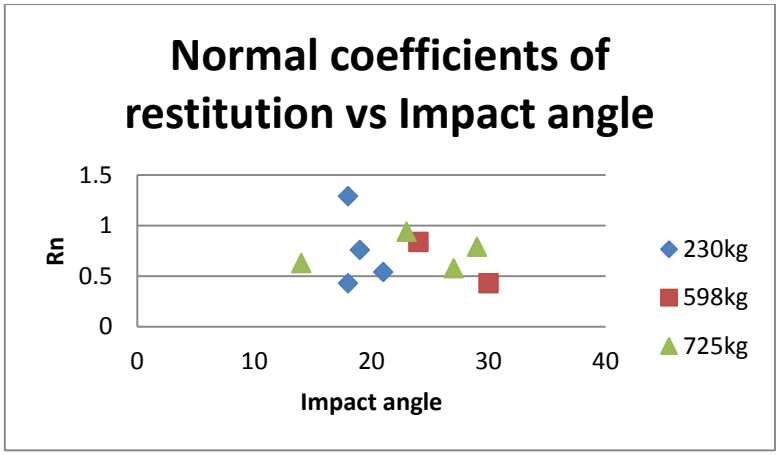

Figure 3-5: Normal coefficients of restitution vs Impact angle; the different colours indicate different masses of boulders

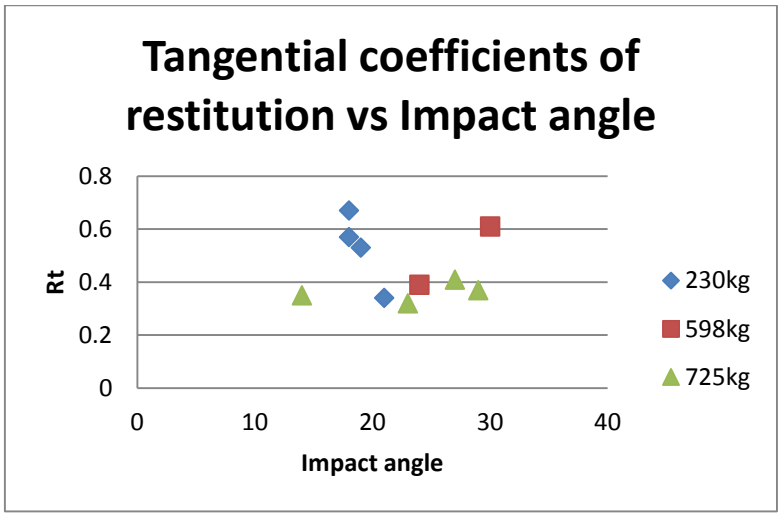

Figure 3-6: Tangential coefficients of restitution vs Impact angle; the different colours indicate different masses of boulders

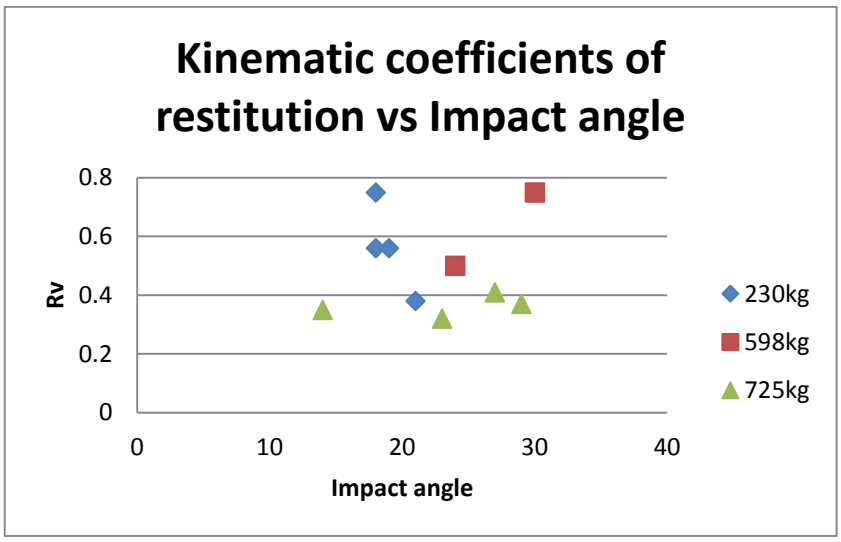

Figure 3-7: Kinematic coefficients of restitution vs Impact angle; the different colours indicate different masses of boulders

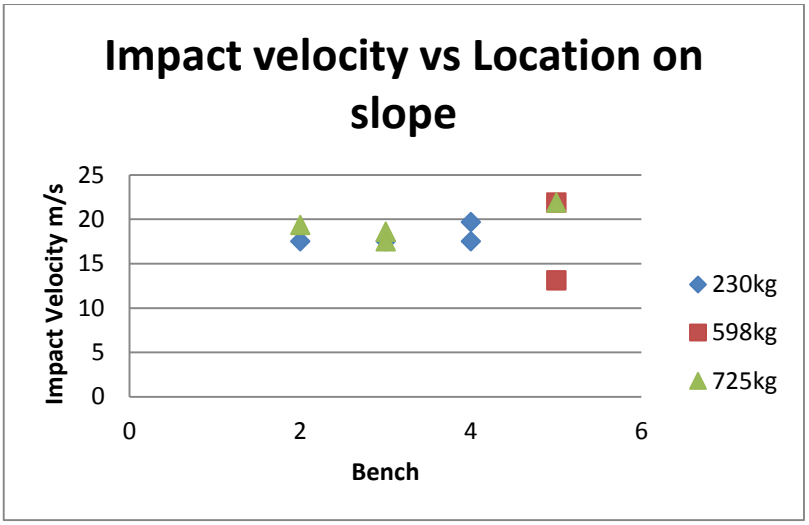

Figure 3-8: Impact velocity vs Location on slope; the different colours indicate different masses of boulders

This led to the idea to plot the impact energy against the slope location, to consider the difference in energy levels, figure 3-9. Surprisingly, the energy levels were relatively constant for the different rock blocks.

The kinematic, normal and tangential coefficients of restitution are plotted against impact energy in figure 3-10 to 3-12, in figure 3-10 there is a divide between the two groups due to the energy levels. However, the second group does not show any coefficient values above unity. In Figure 3-11, low tangential values are indicated, showing that forward movement is highly impeded, with the same groupings as in the previous figure. Figure 3-12, kinematic CoR, follows the same trend as in the previous two figures, indicating that there might be an energy threshold linked to the CoR and all graphs show the same relative groupings. This appears to indicate that the impact energy affects the behaviour of rock-fall trajectory erratically. This might be due to variation in geological media. To investigate this further, data from several publications were tabulated and worked into figure 3-13 (energy specific CoR selection envelope). There are different energy classes in which rock-fall occurs: in low energy regions, elastic to inelastic behaviour can be seen; however, as the energy levels rise, (depending on the rock competencies), the inelastic behaviour becomes more pronounced. The equation shown is the upper limit for the energy specific, CoR, selection envelope.

In figure 3-14, the normal and tangential coefficients of restitution are plotted against the kinematic coefficients of restitution to determine whether there is a relevant relationship. Both correlate well, with the normal CoR showing a slightly weaker correlation. This was improved by removing an outlier, which did not change the equation, only the correlation coefficient.

The equations from figure 3-14 can be used to calculate the correct normal and tangential coefficients of restitution from an impact velocity through the use of the energy specific, CoR, selection envelope in figure 3-13. It is expected that the mathematical expressions will differ from rock type to rock type and also be influenced by geological structure.

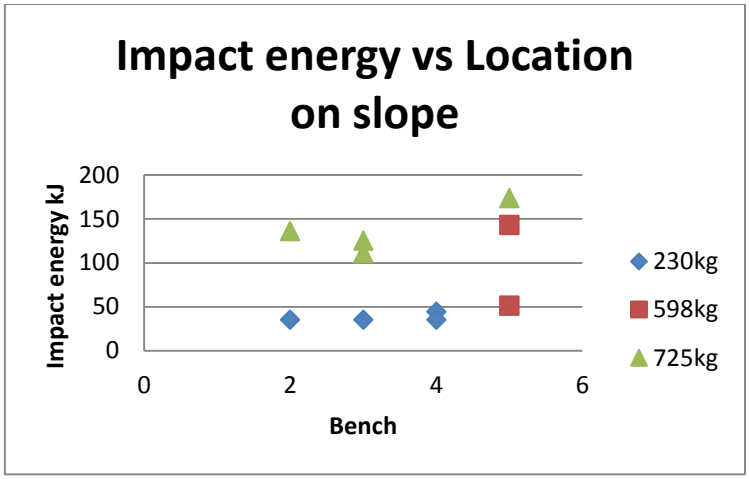

Figure 3-9: The impact energy, and bench location from top down.

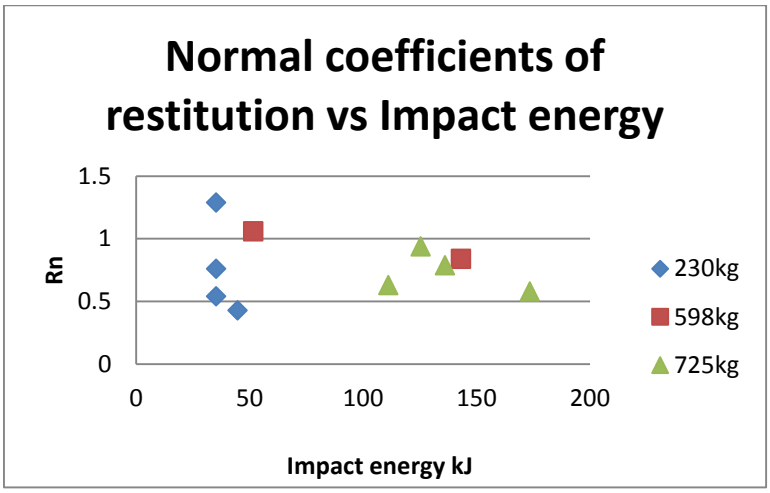

Figure 3-10: Normal coefficients of restitution vs Impact energy; the different colours indicate different masses of boulders

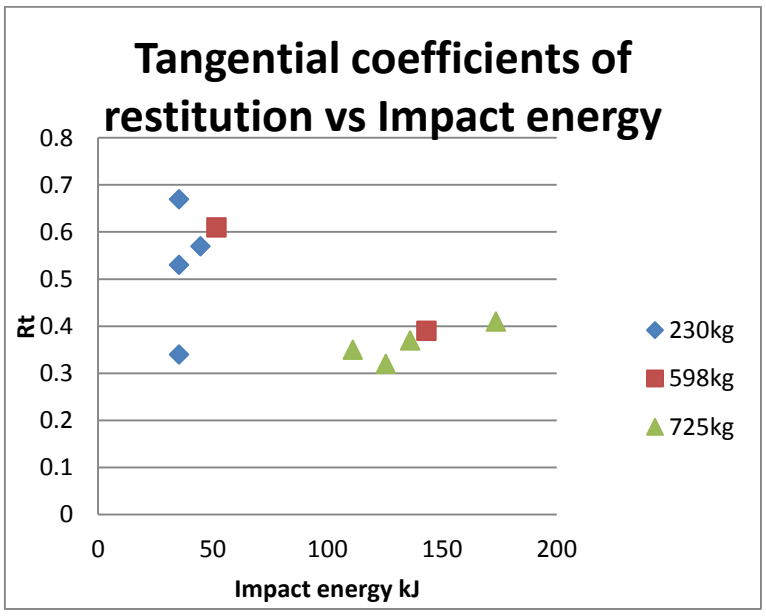

Figure 3-11: Tangential coefficients of restitution vs Impact energy; the different colours indicate different masses of boulders

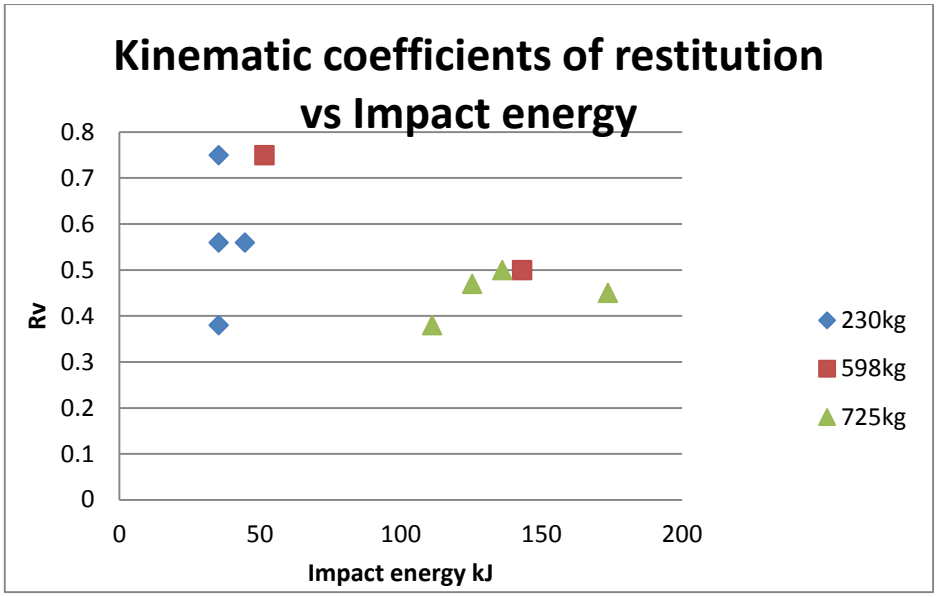

Figure 3-12: Kinematic coefficients of restitution vs Impact energy; the different colours indicate different masses of boulders

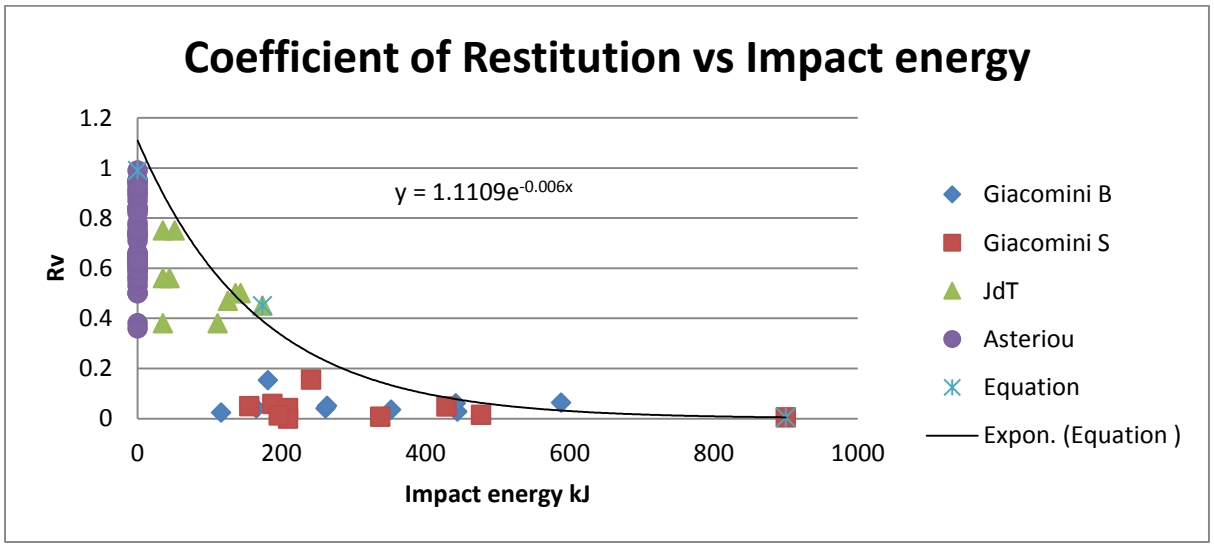

Figure 3-13: The energy specific, CoR, selection envelope

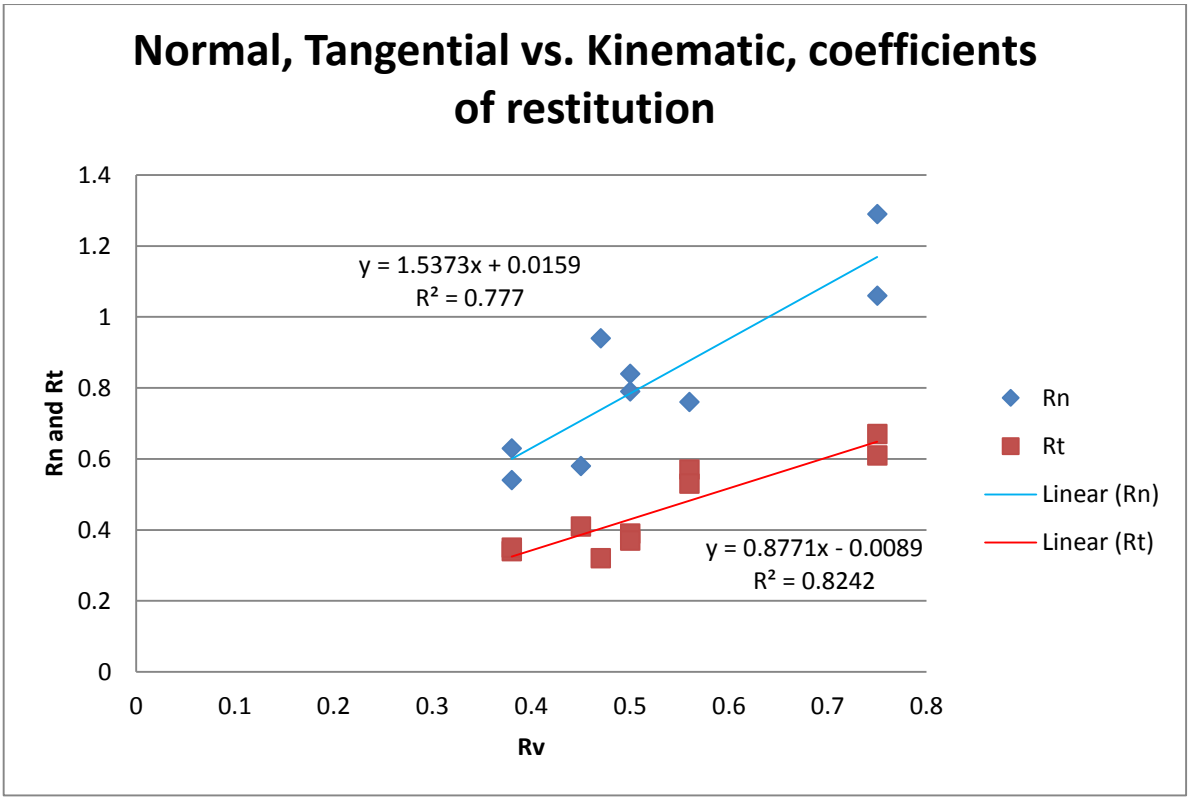

Figure 3-14: Correlation of Normal and Tangential coefficients of restitution with Kinematic CoR

3.5. Summary

The calculated Normal and Tangential Coefficients of restitution do not correspond with values that appear in the literature. In general the Normal Coefficients of restitution are smaller than the Tangential Coefficients of restitution, but this study indicates the contrary.

There is a good negative exponential relationship to the upper-limit of the Kinematic CoR vs impact energy graph. There are also reasonable linear relationships between the Kinematic CoR and the Normal and Tangential Coefficients of restitution. The energy specific, CoR, selection envelope (figure 3-13) and the Kinematic CoR vs Normal and Tangential Coefficients of restitution relationships (figure 3-14) are used later in the site specific rock-fall model.

In Chapter 4, a commercially available software package is used to obtain a calibrated rock-fall model, to compare to, the research rock-fall model in Chapter 6.

Chapter 4

Rock-fall Model Calibration

In Chapter 3, the rock-fall tests data and subsequent, interpreted results from the tests were presented. A negative exponential relationship between the impact energy and the kinematic CoR was discovered from the results (figure 3-13). Further, there are also linear relationships between the kinematic CoR and both the normal and tangential CoR's (figure 3-14).

The results of various attempts to calibrate rock-fall computer models using the rock-fall trajectories determined from the in-situ rock-fall tests conducted at Mogalakwena Mine are described in Chapter 4. In this modelling, Rocsience software, RocFall^{TM} V.4, was used to calibrate the software to the in-situ tests.

4.1. Model Settings

Input data for the computer modelling, as shown in Table 4-1, included estimated values as well as the average values for the Normal Coefficients of restitution and Tangential Coefficients of restitution calculated from the in-situ rock-fall testing. The slope cross-sections were generated from surveyed data from the test sites using AutoCAD, as shown in figures 4-1 and 4-2. The further input parameters were:

Project settings

- 1000 throws

Seeder

- 4m from the top crest elevation.
- Horizontal velocity is 1m/s.
- Rock mass of 675kg.

Table 4-1: Material properties inputs into Rocfall.

Material type	Coefficient of Restitution		Standard deviation	Friction angle	Standard deviation	Slope roughness standard deviation
	Rn(Normal)	Rt(Tangential)				
Rock Slope (Guessed value)	0.487	0.910	0.04	32°	1°	2°
Soil (Guessed value)	0.393	0.567	0.04	20°	2°	2°
Calculated (field test)	0.78	0.44	0.04	32°	1°	2°

In table 4-1, the Calculated (field test) values are the average values that were obtained by averaging the Normal Coefficients of restitution and Tangential Coefficients of restitution values. Values used for the Friction angle, Standard deviation and Slope roughness are typical values for rock and soil. The Standard deviation and Slope roughness values do not influence the trajectory, but introduce variability into the modelling in order to provide a statistical estimation of the slope behaviour (Guzzetti et al., 2002).

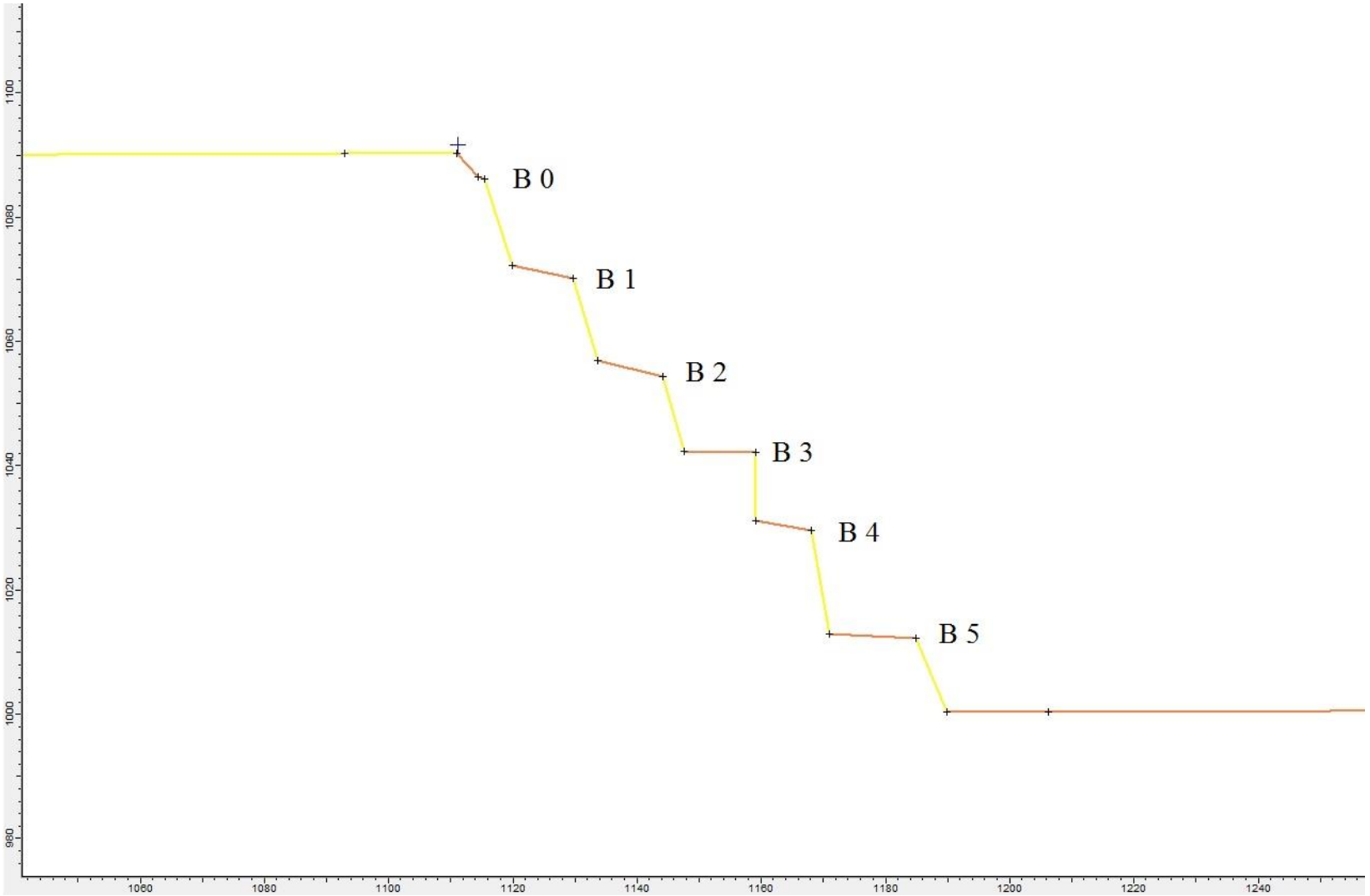

Figure 4-1: Slope cross-section of in-situ test 1, showing bright yellow sections representing clean rock faces and orange sections representing catch berms covered with soil.

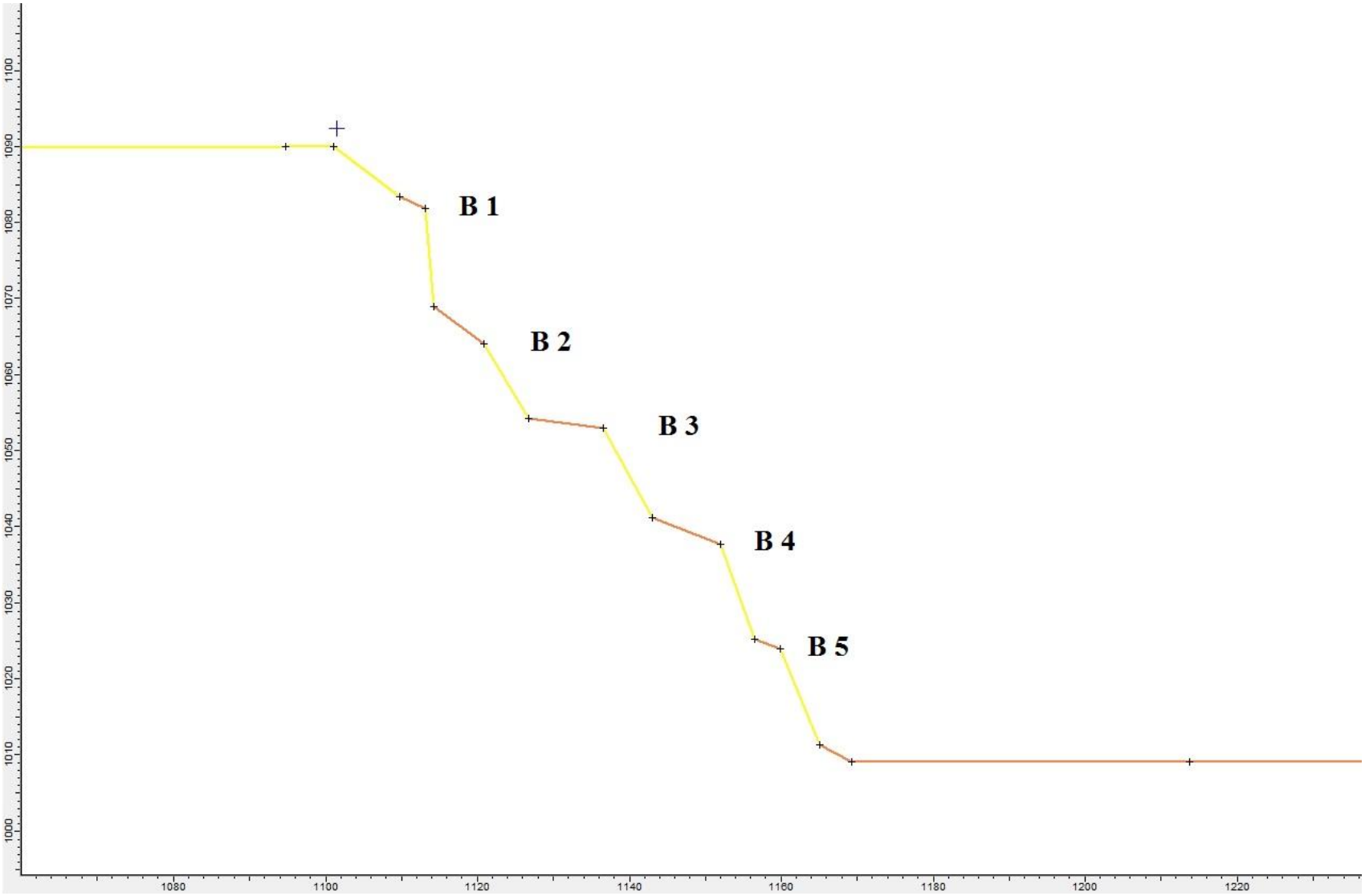

Figure 4-2: Slope cross-section of in-situ test 2 and 3, showing bright yellow sections representing clean rock faces and orange sections representing catch berms covered with soil. In-situ test 2 and 3 has the same cross section due to the little variation when they were initially drawn.

4.2. Results

In model 1 (cross-section at the position of in-situ test 1), input parameters were estimated from the trajectories obtained from the in-situ rock-fall testing. Out of a total of 1000 runs, only 6 runs ended lower down the slope than **B 3**, as was observed in in-situ test 1 (figure 4-3).

In model 2 (cross-section at the position of in-situ test 2 and 3), most of the runs showed the boulder continuing onto the pit floor, as observed in in-situ tests 2 and 3 (figure 4-4). Comparison of the trajectories of the in-situ tests and the rock-fall model shows good agreement.

In figure 4-5, the calculated normal and tangential coefficients of restitution sections are used to simulate the rock-fall. Dull yellow sections (soil) are as in the previous simulation (figure 4-4). Black sections replace guessed rock values with calculated values obtained from in-situ testing.

Comparing the resulting trajectories from calibrated (figure 4-3) and calculated (figure 4-6) at the position of in-situ test 1) many more blocks end lower down the slope than **B 3**.

Comparing the trajectories resulting from calibrated (figure 4-4) and calculated (figure 4-7) at the position of in-situ test 2 there is little difference in the trajectory. The majority of the trajectories do not show impacts on **B 5**.

From the results above, it may be concluded that the calculated values do not correspond completely with the traced trajectories. Nevertheless, the approach is reasonable enough to be used for practical application. What is important to note is that the model includes soft material on bench crests (this enables the dissipation of energy at impact on bench crests due to the lower values of soil).

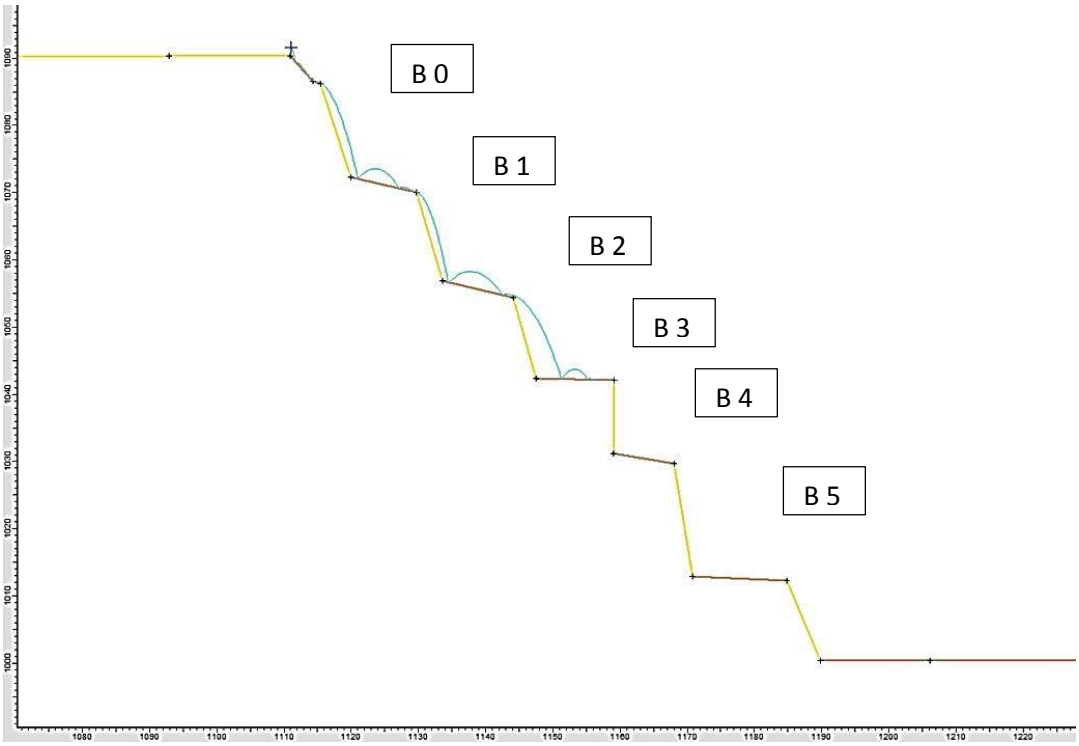

Figure 4-3: Cross-section at in-situ test 1, location.

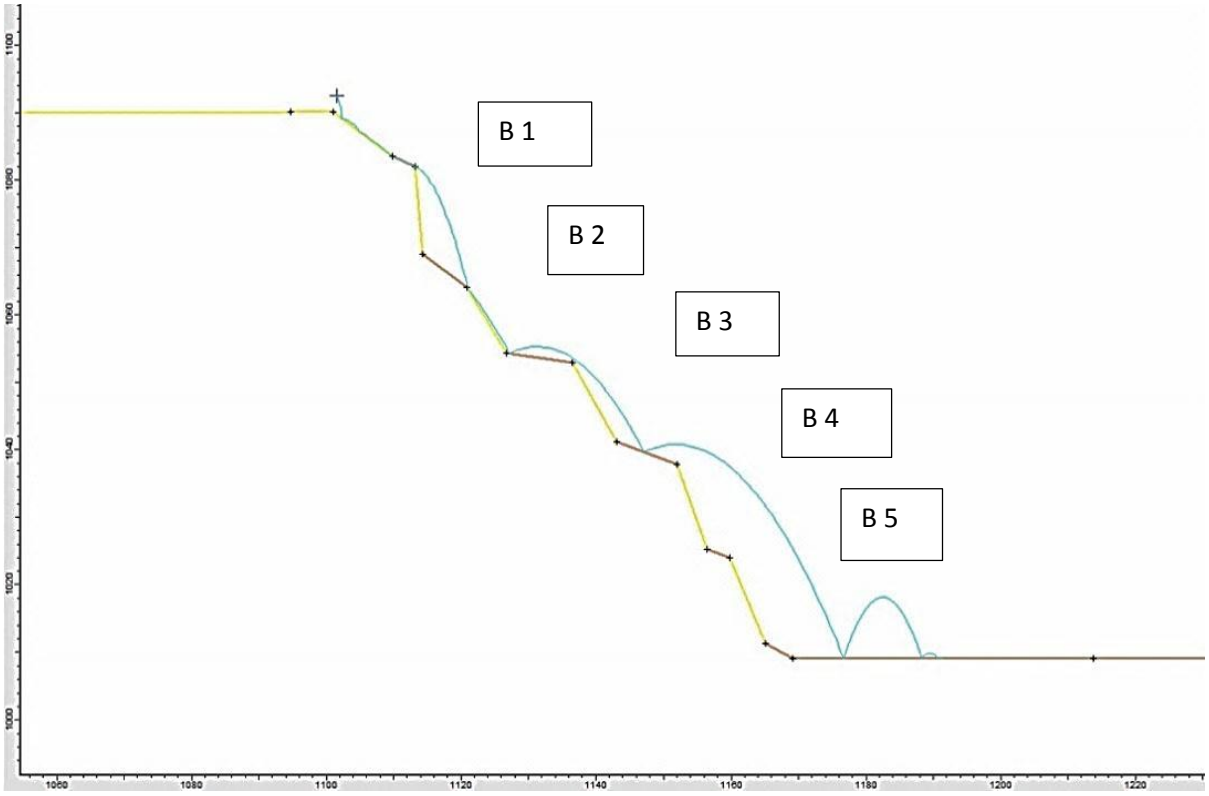

Figure 4-4: Cross-section at in-situ test 2 and 3, location.

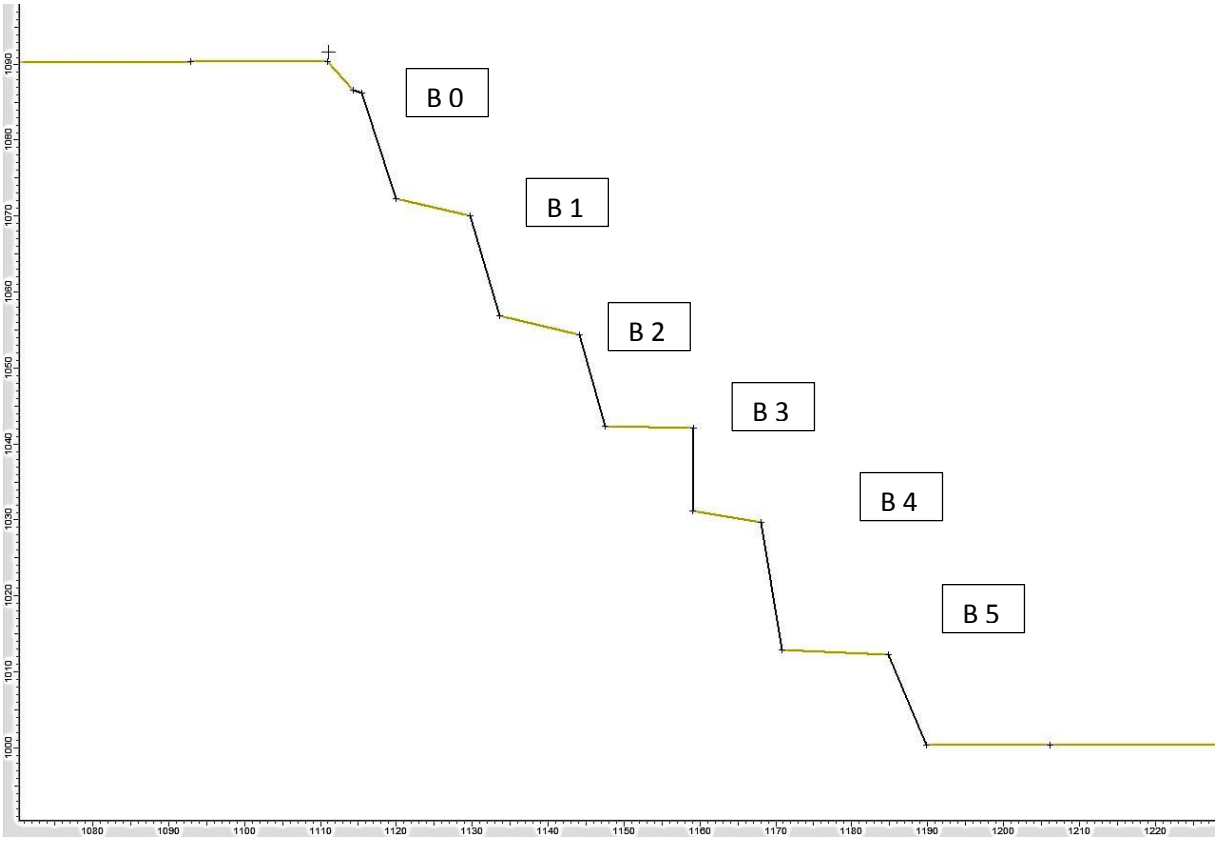

Figure 4-5: Pit section of in-situ test 1, the black sections are the only parts changed from previous rock-fall simulations.

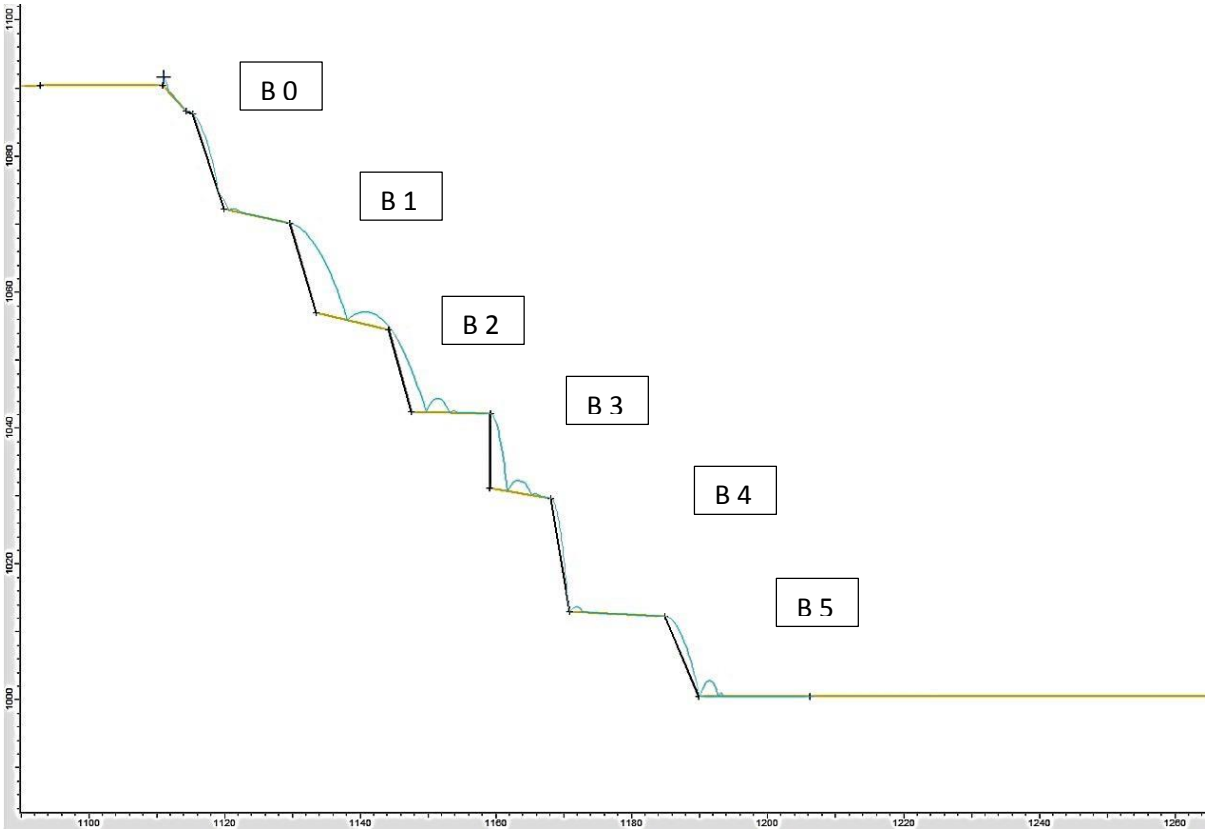

Figure 4-6: Rock-fall simulation done with the rock values calculated from the in-situ test on the profile from in-situ test 1.

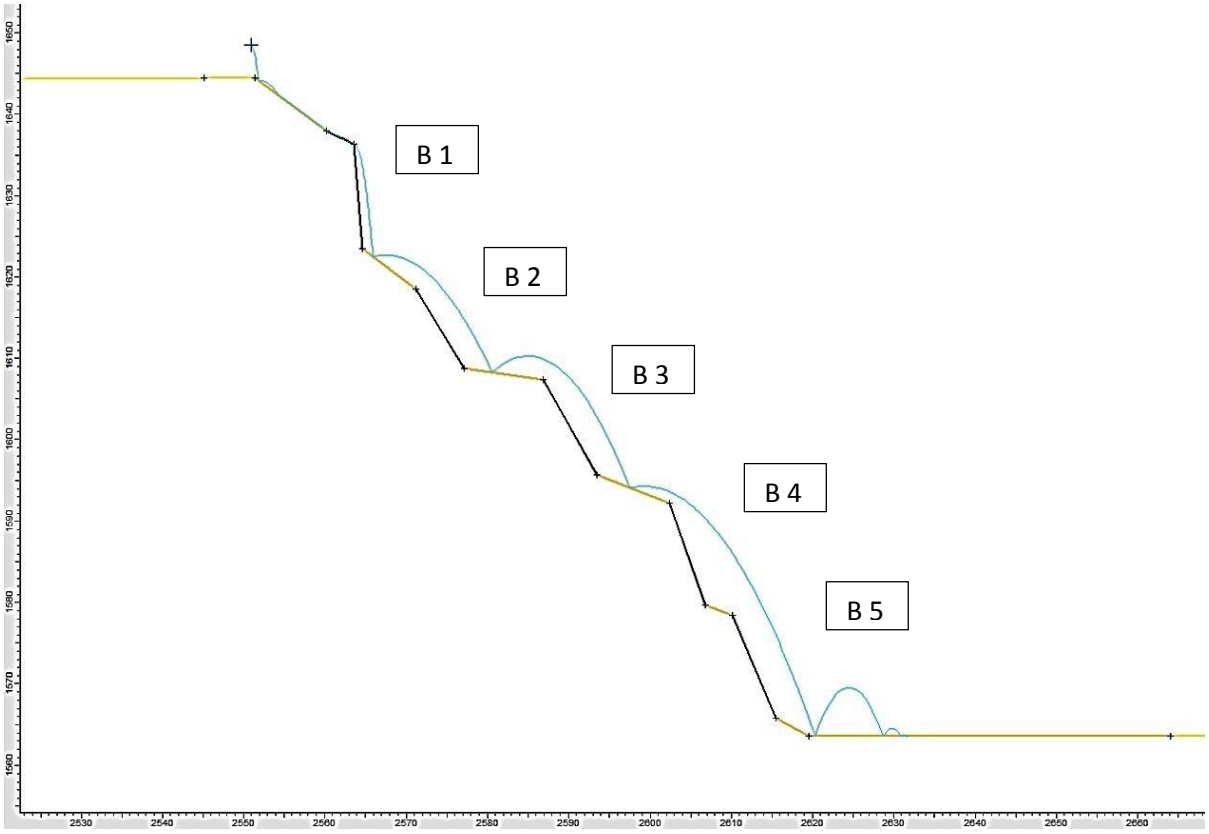

Figure 4-7: Rock-fall simulation done for rock values calculated from the in-situ test on the profile from in-situ test 2 and 3.

4.2.1. Calculated coefficient of restitution

In the modelling described above, no normal CoR scaling was applied within the models. In figures 4-8 to 4-11, a comparison is made between the trajectories using **only** calculated coefficients of restitution **with and without normal CoR scaling**, and a uniform slope material without any "soil areas" on catch berm sections. The effect on the trajectories, with normal CoR scaling, is evident in each case.

The normal CoR scaling damps the normal CoR by an amount calculated using equation 9, given in Section 2.3 (Rocscience, 2003).

Figures 4-8 and 4-9 are based on the cross section profile for in-situ test 1. In figure 4-8, with no damping, the normal CoR gives extremely high rebound trajectories and in figure 4-9, with damping, the trajectories are over damped.

Figures 4-10 and 4-11 are based on the cross section profiles for in-situ tests 2 and 3. In figure 4-10 and 4-11, the outcomes are similar to figures 4-8 and 4-9. From the results of these models it is well illustrated that the normal CoR is over damped and does not give realistic results.

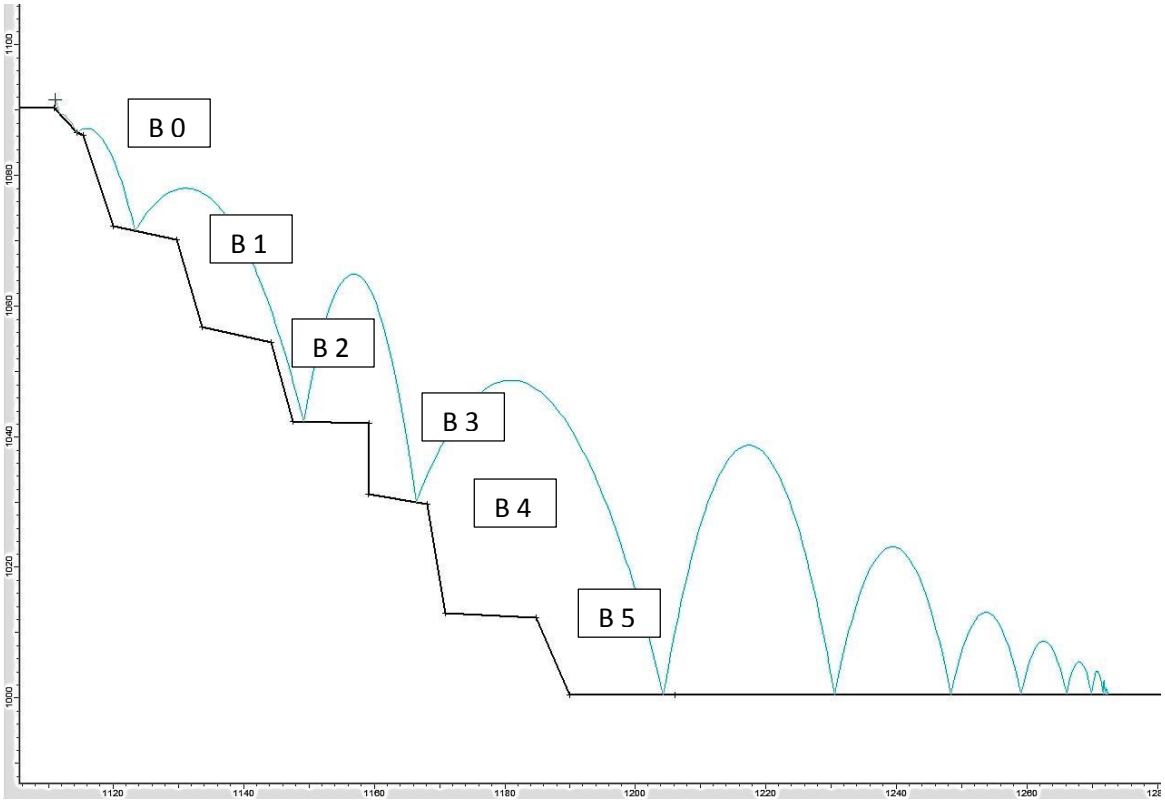

Figure 4-8: Rock-Fall simulations done for calculated coefficients of restitution with no-normal CoR scaling, in-situ test 1 cross section.

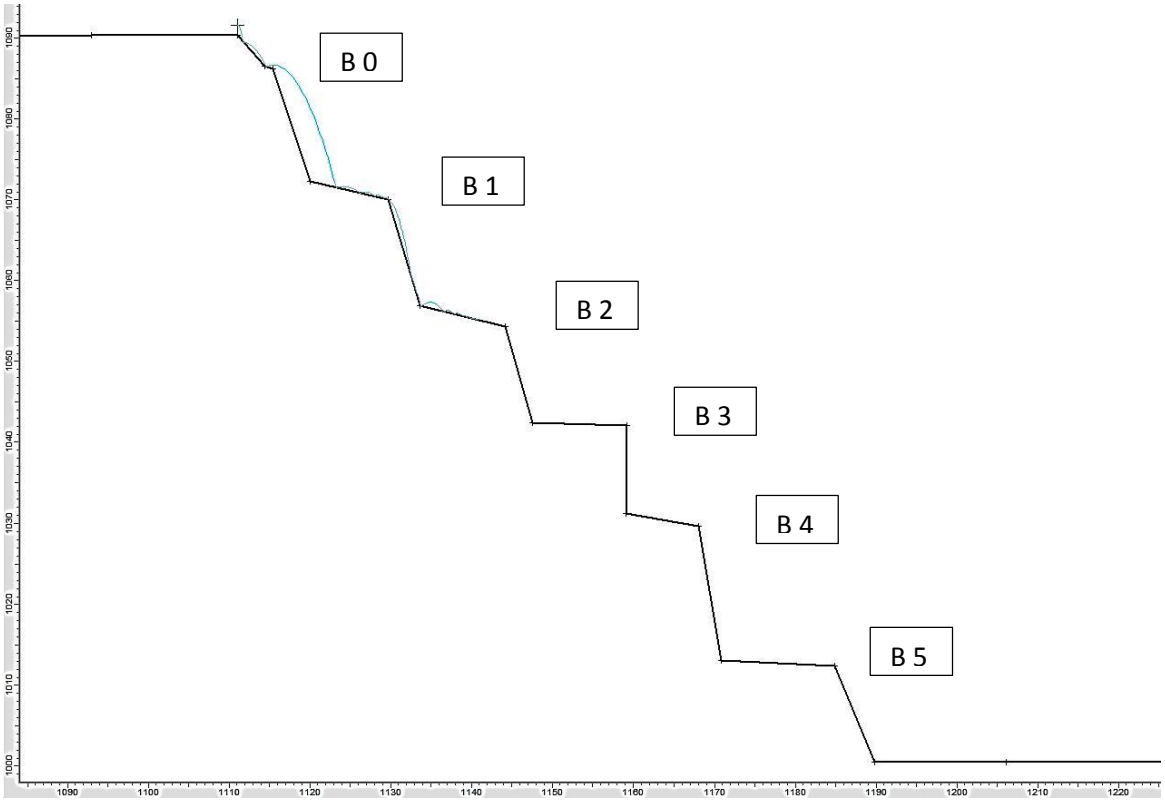

Figure 4-9: Rock-fall simulations done for calculated coefficients of restitution with normal CoR scaling, in-situ test 1 cross section.

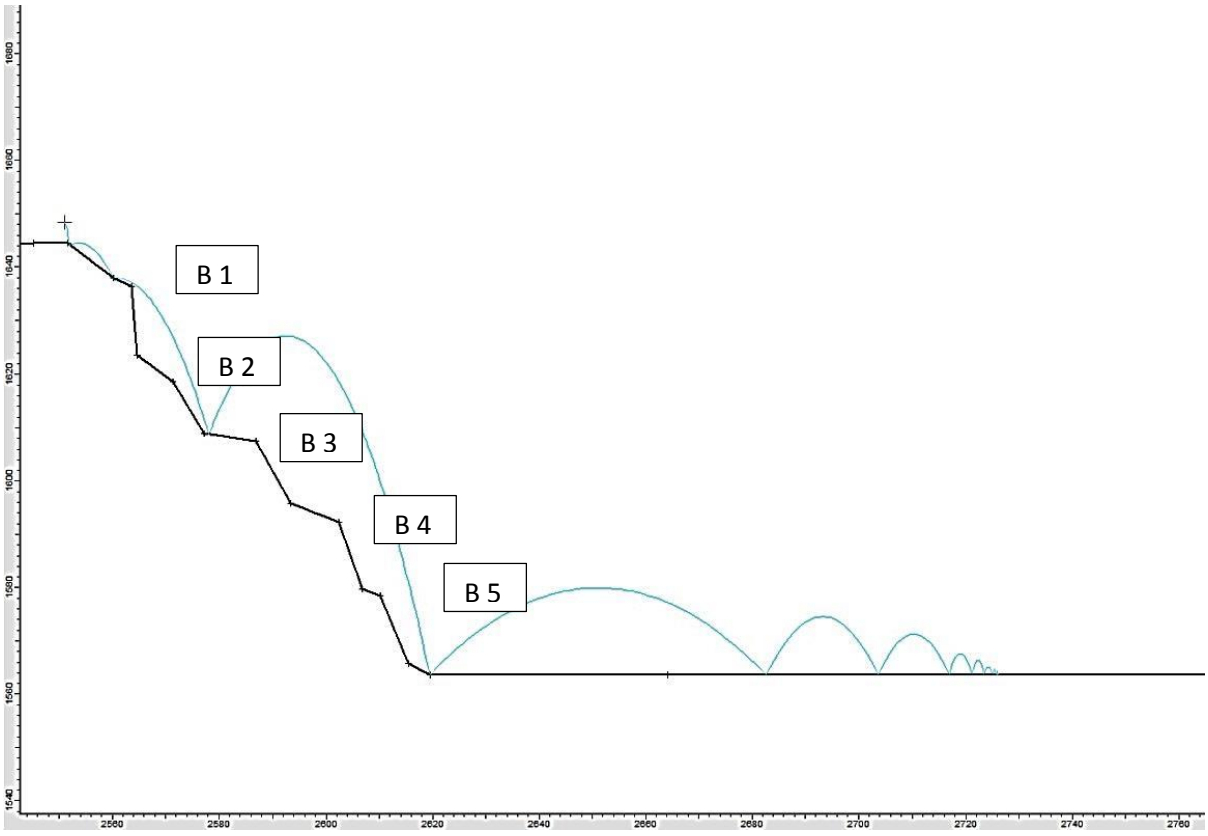

Figure 4-10: Rock-fall simulations done for calculated coefficients of restitution with no normal CoR scaling on in-situ test 2&3 cross section.

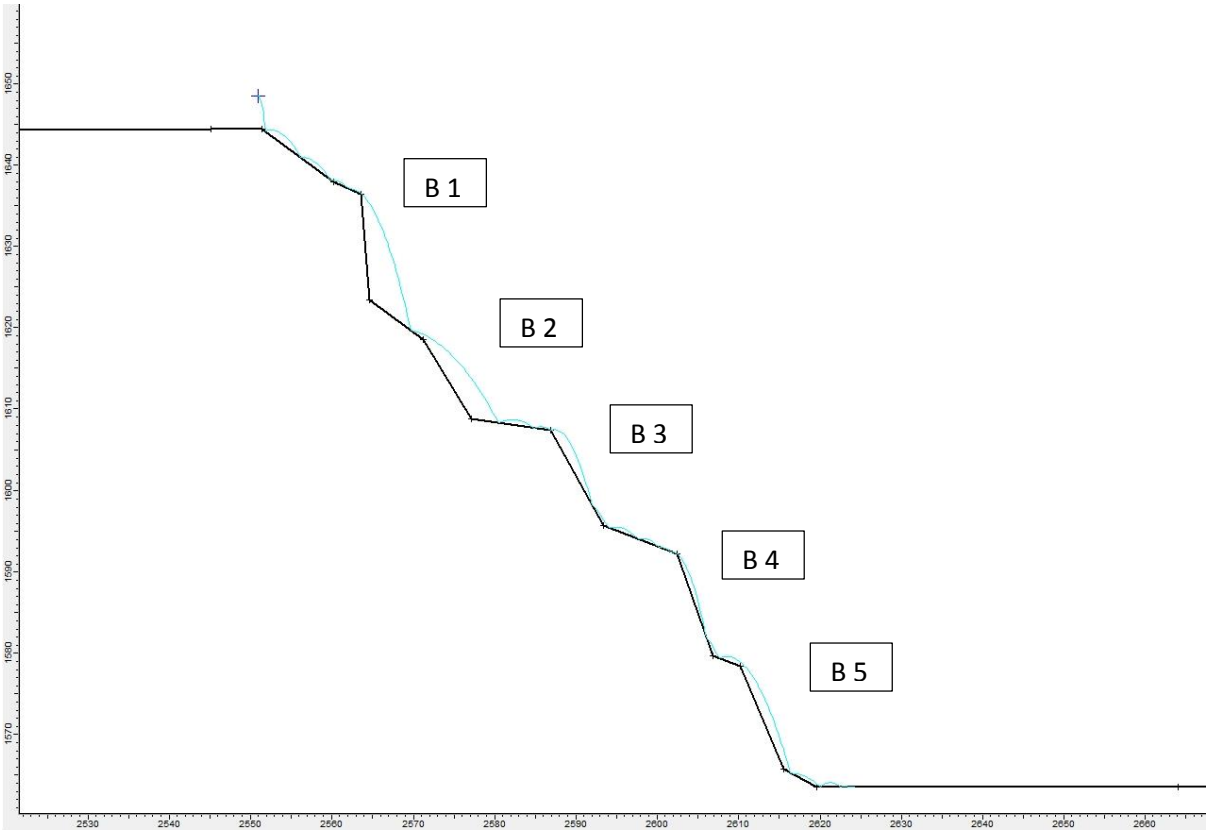

Figure 4-11: Rock-fall simulations done for calculated coefficients of restitution with normal CoR scaling, in-situ test 2&3 cross section.

The best results were obtained by matching the trajectories from the in-situ tests to the trajectories predicted by the software, guessing the material properties, and altering the normal and tangential coefficients of restitution. Using normal and tangential coefficients of restitution calculated from the in-situ testing, and using soil berms to dissipate energy, also produced a good correlation.

This is currently the only way to calibrate rock-fall models, to ensure Normal or Tangential coefficients of restitution are correctly defined. The rock-fall model behaviour is very elastic at the point of impact, due to the calculation method based on stereomechanical impact theory.

4.3. Summary

The two approaches of guessing of the correct material properties from the in-situ trajectories, and calculating the material properties from the in-situ test data, both worked well for the purposes of calibrating the rock-fall model. A significant, negative factor associated with these approaches is that obtaining field test data from boulder tests is difficult and dangerous, which makes this approach not ideal.

Scaling the normal CoR over dampens the trajectories and does not account for energy lost due to impact, and this technique is therefore not recommended.

Laboratory testing can be done to enable the calculation of energy absorption capacity of each rock type and also used to calculate a quasi-static CoR, which can be used in many different applications. This approach is discussed in Chapter 5.

Chapter 5

Laboratory Tests

In Chapter 4, the conventional way to calibrate rock-fall models using results from in-situ rock-fall tests was illustrated, as well as the predicted trajectories from calculated values. It is apparent that many adjustments of inputs are needed before the model is useful.

An alternative approach is one based on laboratory testing of rock samples, which is described in the Chapter. Laboratory tests were conducted to determine the Uniaxial Compressive Strength (UCS) and Energy absorption capabilities of each rock type. The UCS data is used to categorise the rock types into strength categories. The energy absorption capacity values can be used to determine the energy lost at impact. This can be achieved through the use of discrete element modelling as done by Wang and Tonon, (2011). Due to the cost of this software the energy loss was not obtained in this research report.

5.1. Sample Selection

Samples were collected on 1 April 2013. Safety considerations dictated the in-situ locations in this pits from which block samples could be retrieved.

In Mogalakwena North, Central and South, the pits that will be expanded into the super pit, there are three main rock types namely, Granofels (a Granite and Felsic metamorphic hybrid rock), Norite, and Pyroxenite, common igneous rocks encountered in the Bushveld Complex. The following is a brief description of the three rock types:

Granofels:

Granofels is located in the footwall of the pits. It is a metamorphic rock type occurring between the Achaean Granite rock from the Kaapvaal Carton and Felsic rocks from the Bushveld Igneous Complex. It is white and grey-black in colour.

Pyroxenite:

This rock is largely the reef extracted in the middle of the pits along strike. Pyroxenite is an intrusive igneous rock from the Bushveld Igneous Complex. It is dark-grey to green in colour.

Norite:

Norite is located in the hangingwall of the pits. It is an intrusive igneous rock from the Bushveld Igneous Complex with a grey and green matrix.

Two large rock blocks of each rock type were selected and sent to the Genmin Laboratories of the University of the Witwatersrand.

All the block samples were marked with a horizontal line and upward arrow. This enabled the coring of the samples to be done vertically (figure 5-1 A). There is no pronounced layering in the igneous

rocks at Mogalakwena Mine. The approximate depth of the samples was between 50m and100m below surface.

5.2. Sample Preparation

Six rock samples were cored from each rock type with a diameter of 42mm, which was considered to be adequate due to the small grain size of the igneous rocks. The samples were then cut to a length of 110mm and the ends polished to yield a minimum length of 105mm for a width to height ratio of 1:2.5 (figure 5-1 B). The samples' diameter, length and weight measurements were subsequently recorded.

Lateral and axial strain gauges were bonded to the samples and electrical wires soldered to the gauges. Resistance checks were carried out to ensure that the gauges were not faulty (figure 5-1 C).

5.3. Test Procedure

The International Society for Rock engineering (ISRM) has drawn up suggested methods for rock testing (Ulusay & Hudson, 2007). This includes the suggested methods for determining the UCS and deformability (ISRM, 1978), which was followed in the testing of the samples. Specifications include:

Specimen diameter requirements:

- Height to diameter ratio of 2.5-3.
- Diameter approximately 54mm.
- Diameter to grain size at least 10:1.

The 42mm core used was considered appropriate since the grain size was small compared with the diameter.

Specimen ends flatness:

- Flat to 0.02mm
- Perpendicularity to axis no more than 0.001 radians or 0.05mm in 50mm.

Sides of specimen:

- Shall be smooth within 0.3mm over the full length of the specimen.

Capping materials or end surface treatments other than machining is not permitted.

Loading rate:

- The load rate shall be applied constantly that failure will occur in 5-10min.
- Alternatively the stress rate will be within limits 0.5-1.0 MPa/s.

The maximum load will be recorded in kilo Newton to within 1%.

At least five specimens should be tested.

Before the specimens with strain gauges, figure 5-2 A, were tested and results recorded, one specimen of each rock type, figure 5-2 B, was tested to determine a UCS value to estimate the two thirds strength value. Figure 5-2 C shows a sample being unloaded from two thirds the UCS value.

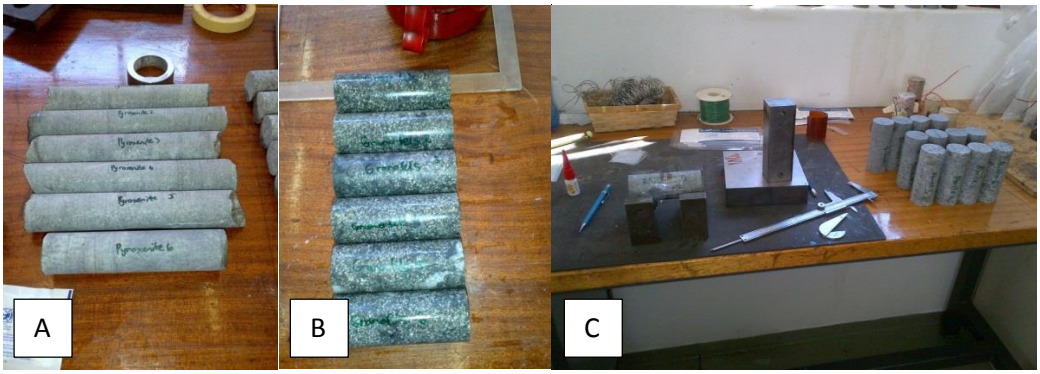

Figure 5-1: A; shows cored Pyroxenite samples. B; Shows Granofels samples cut to 110mm. C; shows the strain gauges being glued to each specimen.

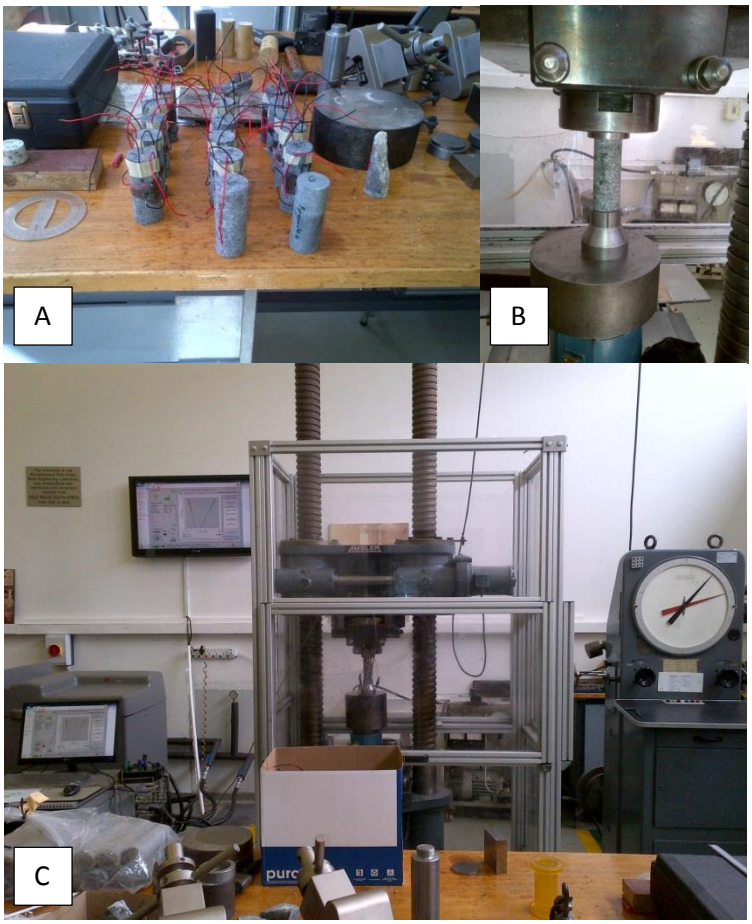

Figure 5-2: A; shows the samples ready for connection to the testing equipment. B; a Norite specimen in place for a Uniaxial Compressive Strength test. C; a UCS test being recorded.

5.4. Energy absorption capacity of each rock type and quasi-static CoR calculations

The data set for each test was loaded into Microsoft excel (figure 5-3) and a 6th order polynomial function was added to the loading (figure 5-4) and unloading (figure 5-5) cycle to get a best fit line to describe each cycle. The polynomial function was then integrated to get the area under the polynomial function, this in turn will give the energy in the sample at the stress applied and the difference in energy was compared for the loading and unloading curve. This was then defined as the quasi-static CoR. There after the same was done with the UCS cycle and the energy absorption capacity of the sample was calculated.

The results are summarised in **Appendix 2**.

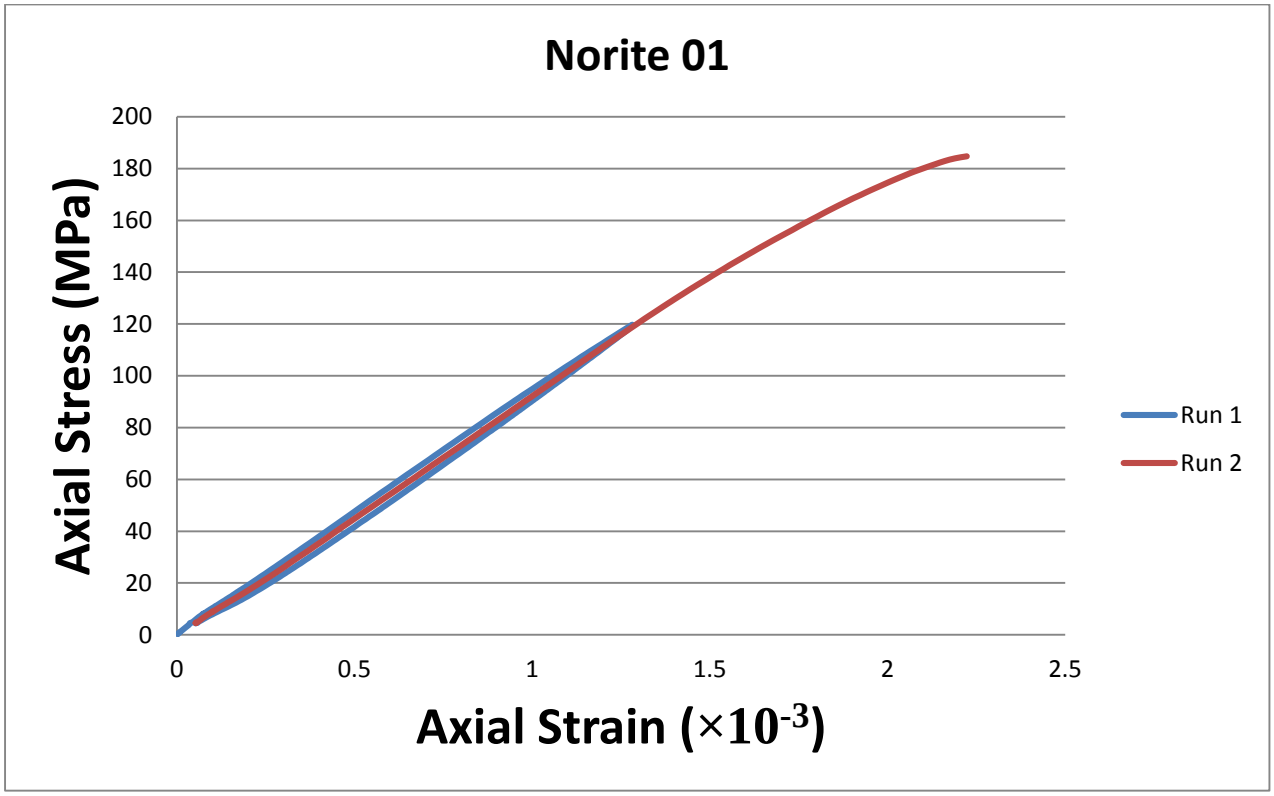

Figure 5-3: A UCS test, with two stress-strain cycles, showing hysteresis, samples was loaded to approximate two thirds of the UCS value before unloading and reloading to failure.

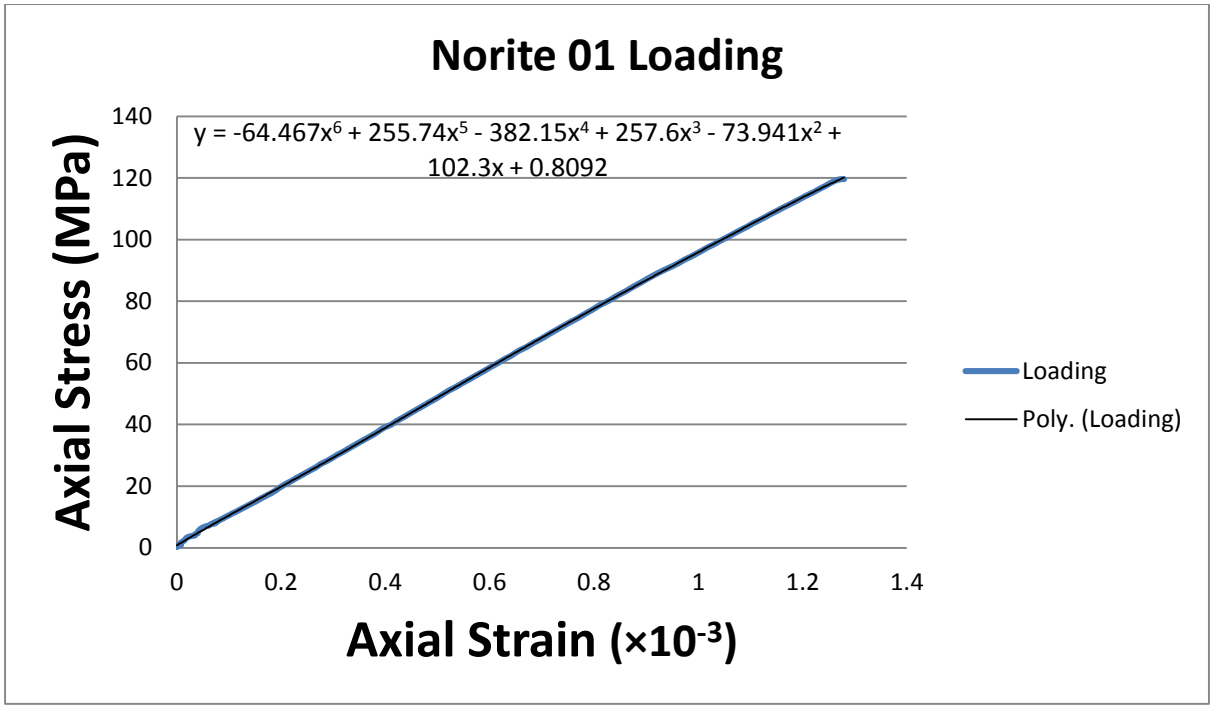

Figure 5-4: The loading stress-strain path with a 6th order polynomial function, describing the shape of the graph. The area underneath the stress-strain graph represents the energy contained within the sample.

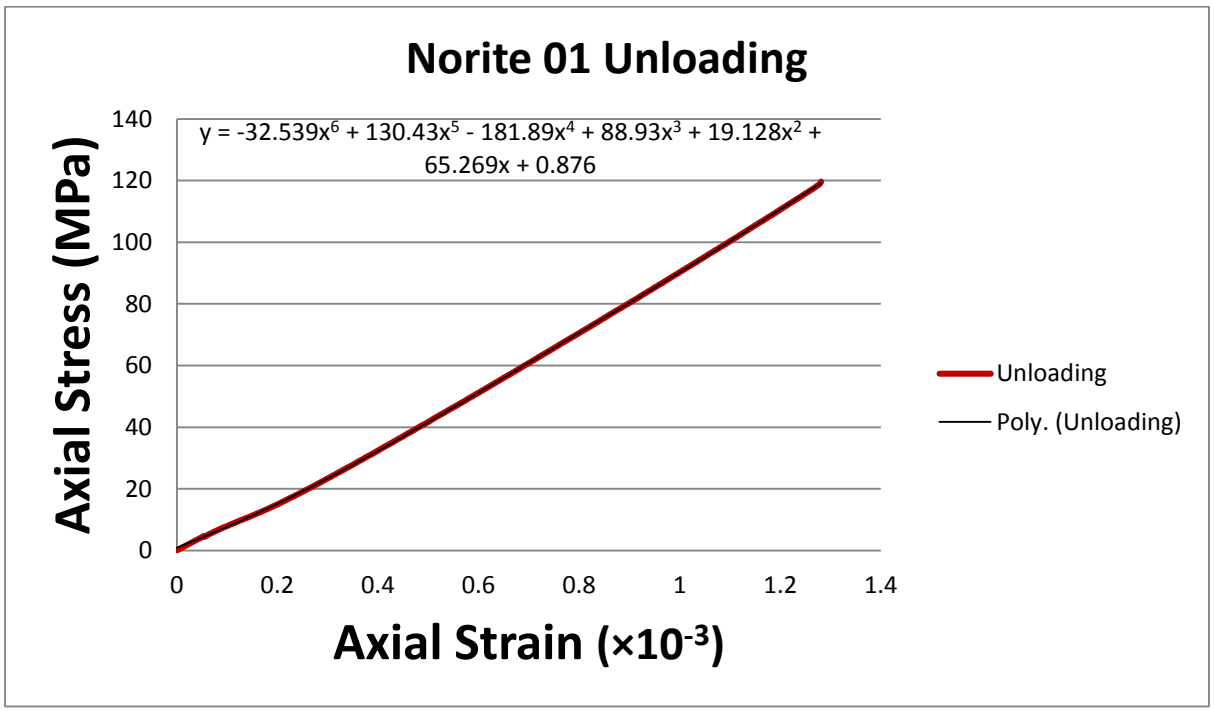

Figure 5-5: The unloading stress-strain path with a 6th order polynomial function, describing the shape of the graph.

5.5. Results

The tests commenced on 10 April 2013. On average each test was completed in 8 and a half minute. The specimens were loaded to two thirds of the expected maximum load, then unloaded to 10kN and reloaded to failure. The laboratory test results are summarised in table 5-1.

Table 5-1: The rock properties obtained for the three rock types through laboratory testing.

Rock Type	Norite	Granofels	Pyroxenite
CoR	0.91	0.94	0.95
UCS (MPa)	177	204	221
Poisson's Ratio	0.34	0.28	0.29
Modulus of Elasticity (GPa)	93	105	100
Energy Absorption Capacity (MJ/m3)	202	220	301

Unfortunately the energy absorption values calculated, **Appendix 2**, could not be used further, since the discrete element modelling software required for the calculation of energy lost at impacts was not available. However, according to Fornaro et al (1990), for rock on rock impact, 60% of the energy is unrecoverable and for soil and debris 75-86%. This will give CoR values of 0.6 (rock on rock impacts), which correspond with the kinematic coefficients of restitution of 0.59 and 0.5 respectively, calculated in in-situ test 2 and 3.

5.6. Summary

Laboratory strength and deformation testing has shown that the differences in mechanical properties of the three rock types are relatively small. For the CoR variation of plus minus 0.02, the calculation method of rock-fall is not precise enough to differentiate between the behaviours of the three rock types tested.

The UCS values will help to identify within which hardness range different rock types belong. For the values obtained from the laboratory testing it is evident that Mogalakwena rocks fall into the very hard rock category.

In the following chapter, Chapter 6, the concept of the site specific rock-fall model, based on the energy specific selection of the kinematic CoR, is explained.

Chapter 6

Site-specific rock-fall model

In Chapter 5, the results of rock property tests were presented, showing that there is very little variation in the fresh rock at Mogalakwena Mine in terms of rock-fall simulation properties.

In this chapter an attempt is made to use a rock-fall model, based on the research (Research rock-fall model) carried out to simulate conditions at Mogalakwena Mine. In the research model, no frictional effects are taken into account, and at impact, the initial velocity determines the Kinematic CoR. The corresponding normal and tangential CoR values are then predicted for the specific impact. The free fall and rotational equations used to calculate the energies are taken from Giancoli, (2005). At present there is no international standard in the study of rock-fall to govern rock-fall motion or in-situ testing (Giani et al., 2004).

It is expected that it will be possible to expand the model to cater for different rock-fall conditions, when further CoR versus impact energy graphs, catering for different rock strengths, have been prepared. One will be able to select the applicable graph according to the UCS of the specific rock. The CoR behaviour will then correspond to the selected graph, according to the impact energy range that corresponds to the individual impact as being calculated (refer to figure 3-13 for the energy specific, CoR, selection envelope). Figure 6-1 shows examples of such envelopes. This can be an additional feature in rock-fall software to be able to accurately simulate rock-fall without time-consuming and potentially dangerous in-situ calibration.

In the flow diagram below, figure 6-2, the proposed method for calculating rock-fall trajectories is shown. In figure 6-3 and 6-4, the trajectories from the rock-fall calculations are based on the process outlined in figure 6-2. The calculations are carried out using the equations from Giancoli, (2005), within the text book the equations are from chapters 3, 6 and 8. The relevant equations used are given in **Appendix 3**. All the calculations done to generate the research rock-fall model are shown in **Appendix 4**, an excel spreadsheet. There is no frictional or sliding component in the research rock-fall model.

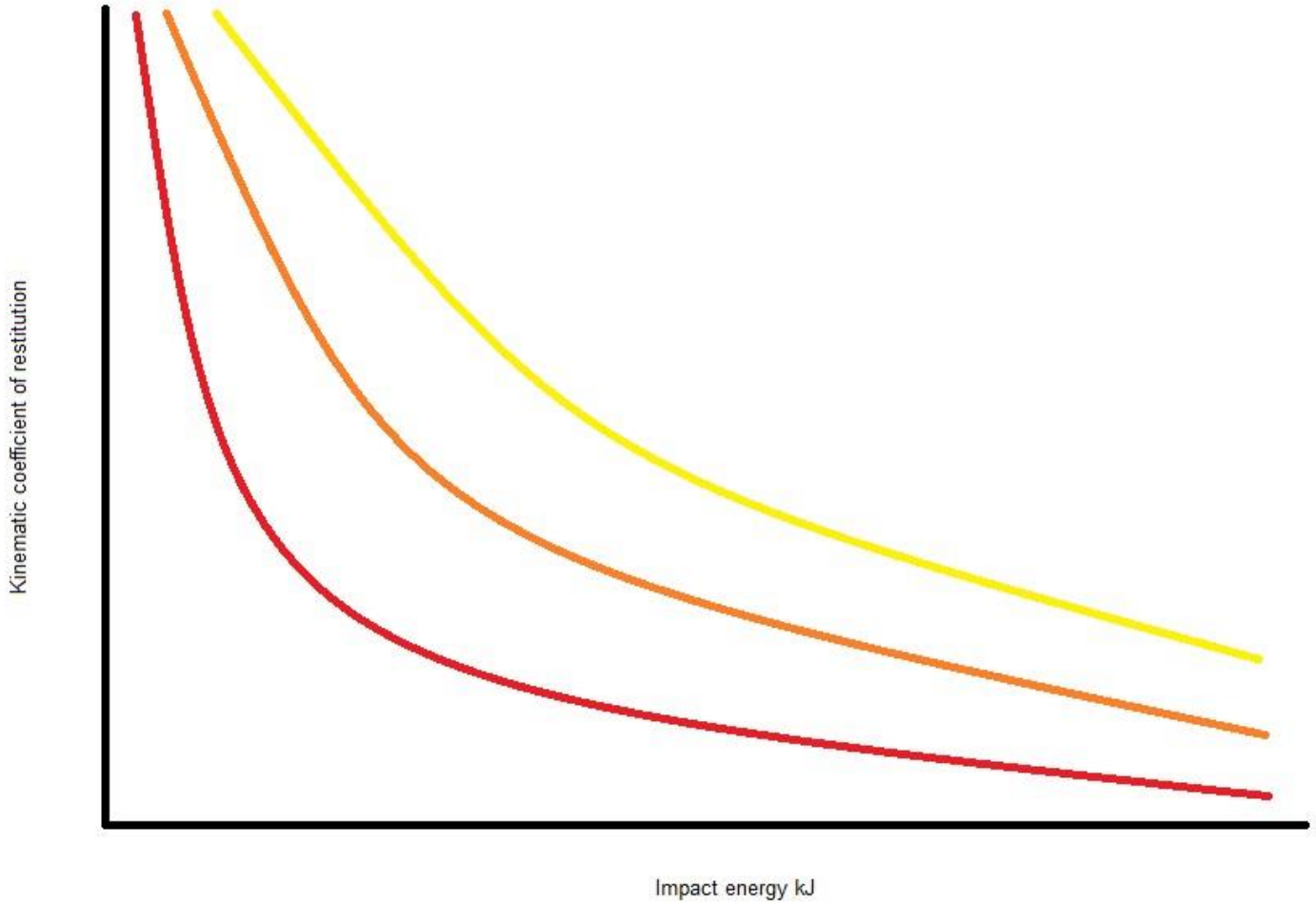

Figure 6-1: Proposed energy specific CoR selection graph, per rock strength category, each colour representing a different UCS value.

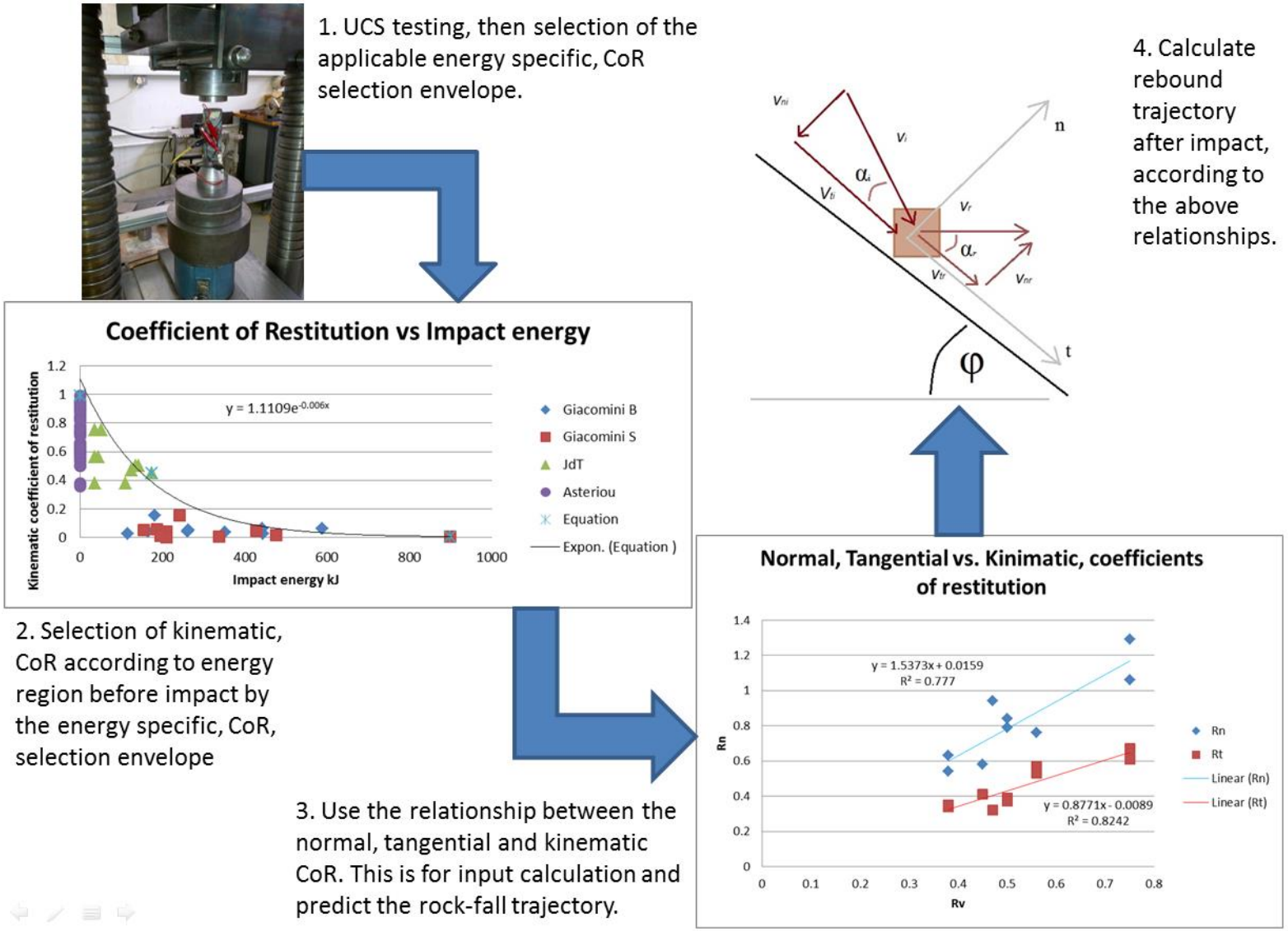

Figure 6-2: The flow diagram shows the process that is used to calculate the site specific rock-fall model trajectory

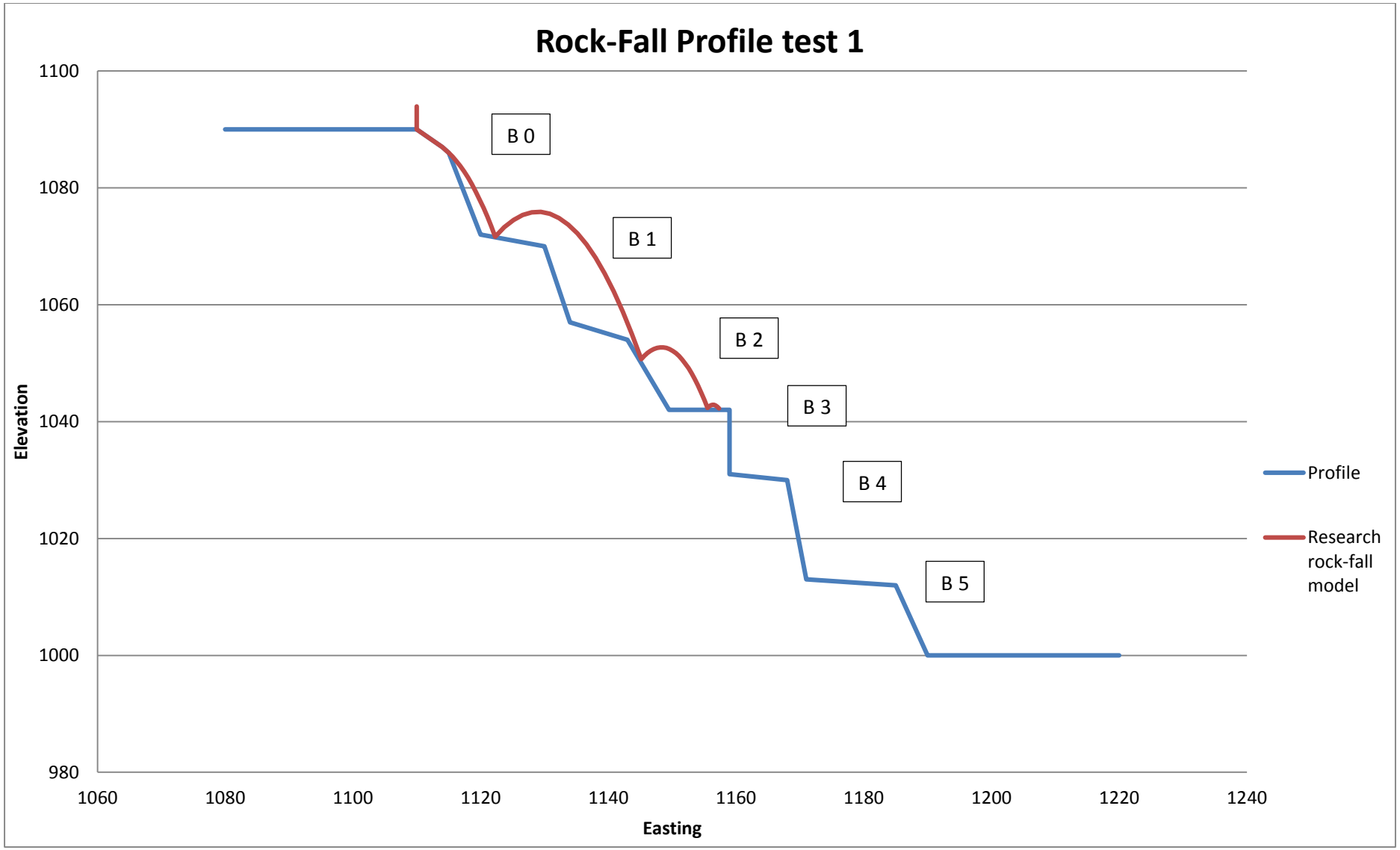

Figure 6-3: Calculated rock-fall trajectory from data obtained through the study, for the first test site, using the research rock-fall model

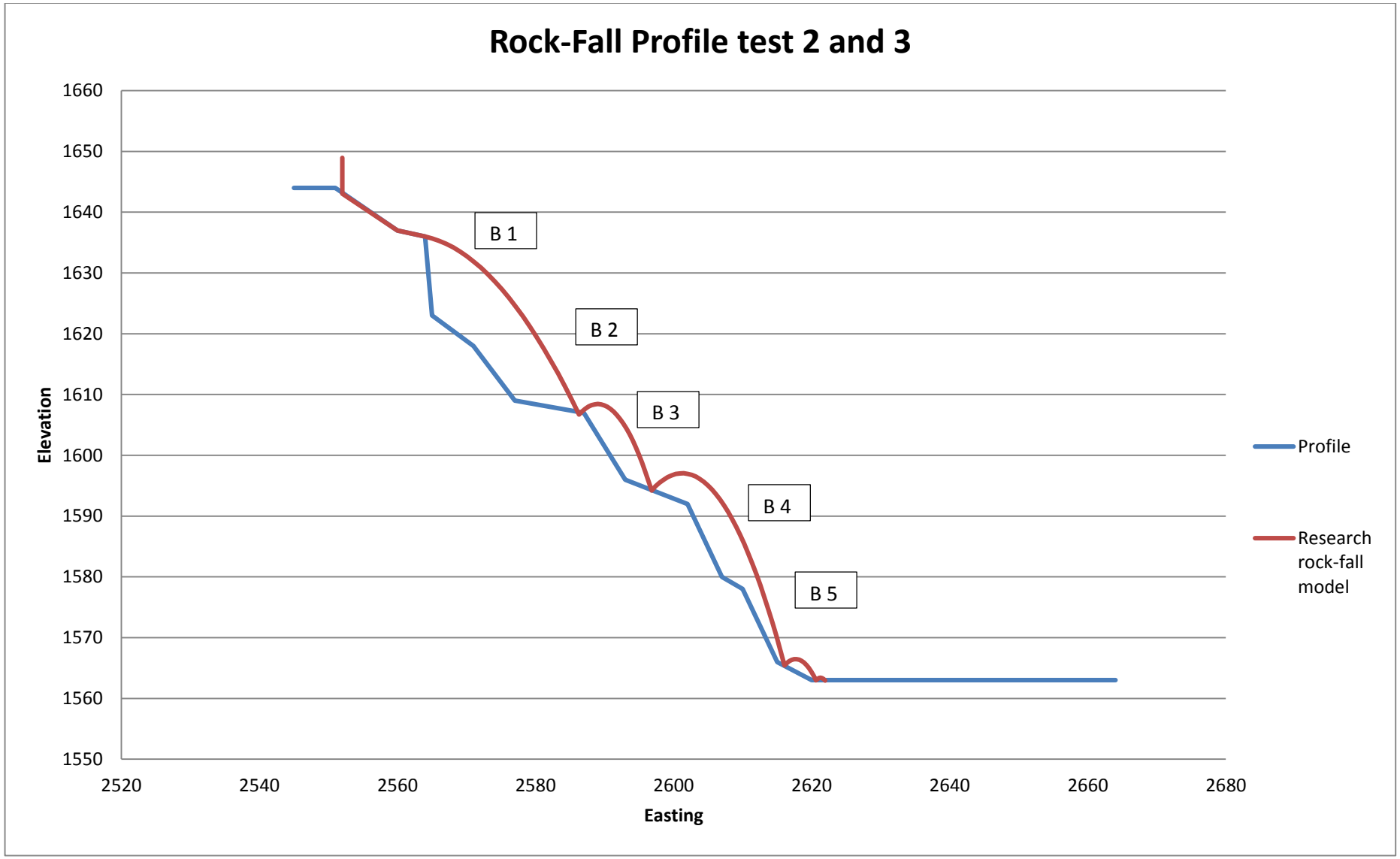

Figure 6-4: Calculated rock-fall trajectory from data obtained throughout the study, for the second and third test site, using the research rock-fall model

6.1. Comparison

The output from the research rock-fall model (site specific rock-fall model), and the results of the calculated values (from the rock-fall trace Chapter 4) used in Rocfall^{TM}, (Normal and Tangential coefficients of restitution, Section 4.2.1.) with no soft material (figure 4-8 and 4-10), only hard rock in the profile, are compared in figures 6-5 and 6-6. The high jumps in figure 6-5 and 6-6 is due to the average Normal and Tangential coefficients of restitution used coupled with, no "soft" areas to dissipate energy out of the rock-fall system. Thus one gets elevated bounce highs as discussed in Chapter 4.

The in-situ traces from in-situ tests 2 and 3 are also included, it may seem that the traces are rebounding off air and not a solid surface, this is due to the difficulty of finding the precise profile where the tests were carries out. It is evident that the dynamic selection of the CoR, in the research rock-fall model, results in realistic predictions of rock-fall trajectories. These results illustrate the potential of the site specific rock-fall model approach described for calculating rock-fall trajectories. However, enhancements of the model need to be implemented to improve the accuracy of predicted rock-fall trajectories even further, and these are the inclusion of friction, and statistical variability.

Commercial software such as Rocfall^{TM} predicts the trajectories very well when it is calibrated to in-situ traces. However this is a very unpopular procedure in a mine where space is limited and equipment required for the tests is not readily available. In addition there is the risk that these tests pose to the operation - delays in production and safety concerns, making the in-situ testing approach unattractive. The research rock-fall model approach is therefore an attractive alternative.

6.2. Summary

Rock-fall can be calibrated to correspond with an observed trajectory; this however introduces an element of doubt as to whether a bias is being built into the modelling in order for the software to generate a trajectory that is desired. The question which arises is whether this calibrated model will provide realistic rock-fall trajectories for a different location.

The Calculated CoR values (section 4.2.1.), used as inputs to the software with a uniform slope, with no "soft" areas to absorb energy out of the system, show unrealistic trajectories in figures 6-5 and 6-6. In contrast, the energy specific CoR selection envelope (ESCORSE), (figure 3-13) used to calculate the trajectory named "Research rock-fall model" (with a uniform slope with no "soft" areas to absorb energy out of the system) closely follows the actual in-situ trajectory observed in the testing done on site.

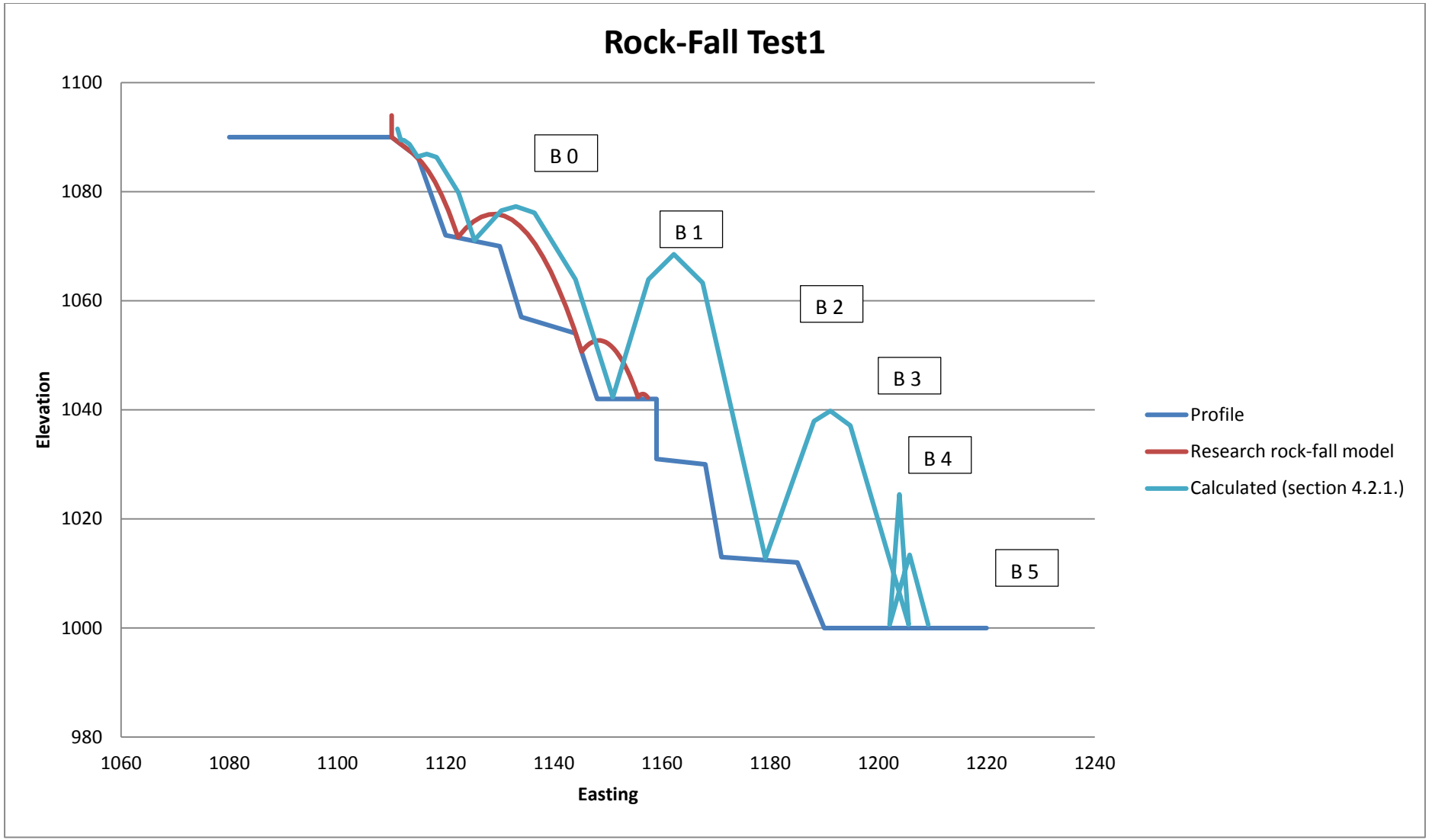

Figure 6-5: Rock-fall test 1, slope profile: comparison between the calculated coefficients and site specific rock-fall model. There was no in-situ trace for test 1, however the rock-fall stopped on geotechnical catchment of B 3, as in the in-situ test. The trajectories were scaled to correspond with the cross section.

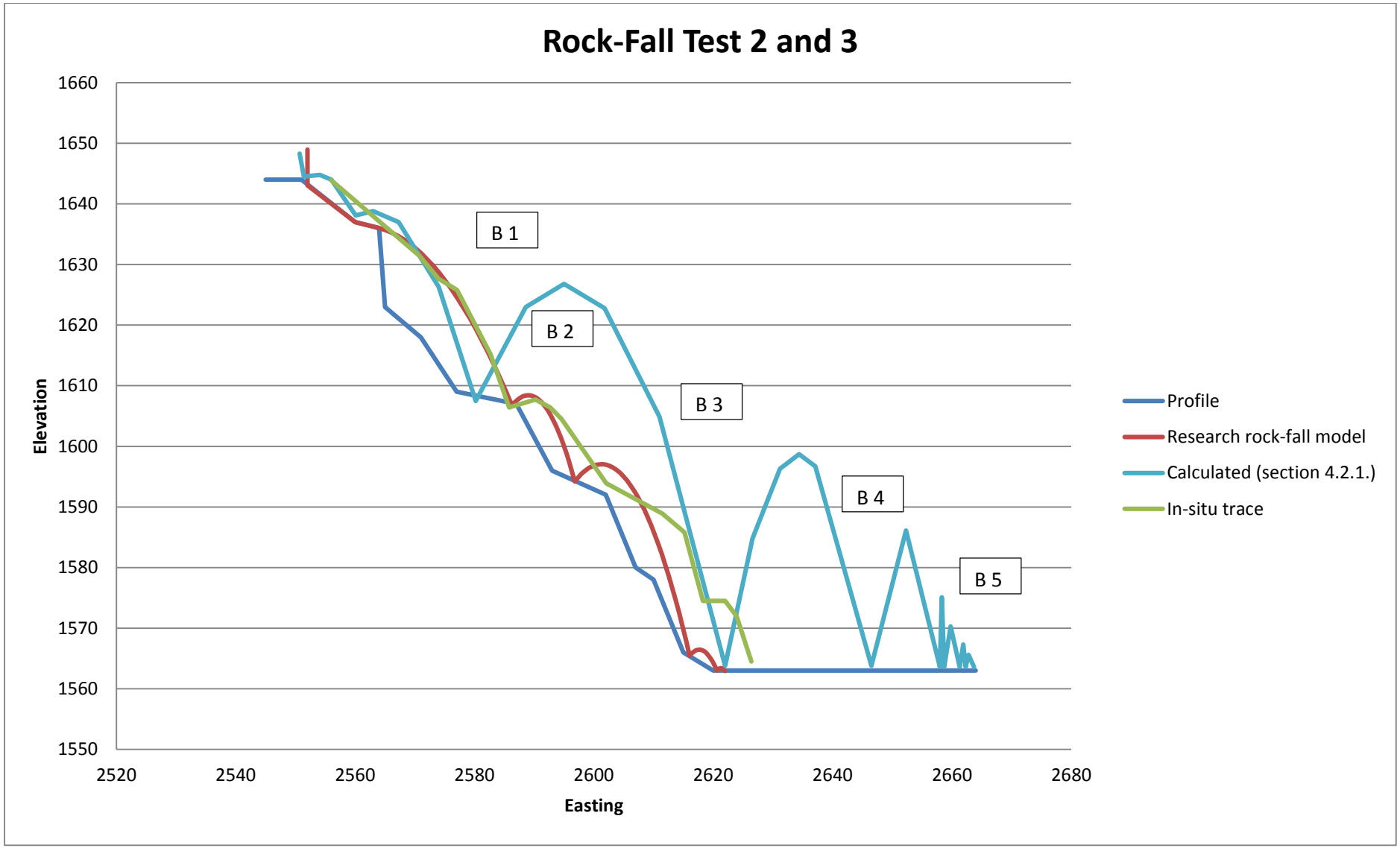

Figure 6-6: The comparison for in-situ rock-fall test 2&3 trace, calculated coefficients and site specific rock-fall model. The trajectories were scaled to correspond with the cross section.

Chapter 7

Summary and Conclusions

Rock-fall studies are mostly focused on geomorphological studies and civil construction projects with limited study in mining. These studies developed techniques that are very useful in operational environments where over design is used to eliminate risk caused by hazards such as rock-fall.

In open pit mining, optimal design of catch berms based on accurate rock-fall modelling is vital. Sufficient catchment (spill berms) must be designed into open pit slopes to ensure the safety of working personnel. Conditions may arise during the operational life of open pit slopes where the planned design is not fully achieved. Under and over mining of the catchment design may lead to increased risk, both with regard to employee exposure and economics.

Civil engineering approaches are often very conservative that result in very costly preventative measures due to the "over design" of these measures. More accurate rock-fall modelling may help to reduce the cost in these systems without exposing people to higher risk levels.

There are numerous ways to assess the level of rock-fall risk. One of the best known is the RHRS (Rock-fall Hazard Rating System of the California Department of Transportation) modified to open pit mining design. The system may be used to identify risk severity and possible support type solutions. Proposed support is then examined within rock-fall trajectory simulations.

Rock-fall simulations assume inelastic impact behaviour (stereomechanical impact theory). The Coefficient of Restitution (CoR) sets the limit to energy loss within the simulation. Kinematic CoRs are determined through height, velocity or energy. The Kinematic CoR is split into vector components (Normal and Tangential CoR) for application into modelling software. Current on-site software uses an average CoR parameter based on a normal distribution for variance. This does not predict the observed rock-fall behaviour satisfactorily.

From field tests, Kinematic, Normal and Tangential CoR values were calculated from velocities before and after impact. Three vital relationships were established - a negative exponential correlation was found between the impact energy and Kinematic CoR, known as the energy specific CoR, selection envelope (ESCORSE); and linear correlations between the "Kinematic CoR and Tangential CoR" and "Kinematic CoR and Normal CoR".

This study shows that the CoR varies under different impact energy levels. Different CoR values are selected for impact specific energy level, which then allows better prediction of the rock-fall trajectory. A close correlation exists between the in-situ traces observed and the predictions from the research rock-fall model. The research rock-fall model has demonstrated the ability to predict rock-fall trajectories with greater accuracy.

The calculated values were also used in conventional software to compare the conventional approach to the site specific rock-fall model. It was shown that when the calculated values are used without adding additional damping zones (soil sections on geotechnical catchment berms) the rock-fall simulations were unrealistic.

Additionally, the outlined process allows for UCS results to be used for selecting appropriate input (energy specific, CoR, selection envelope). This simplified approach eliminates the need for the in-situ calibration tests that pose high risk to mining equipment and personnel.

The site-specific rock-fall model can be adapted to suit any geological environment with the use of discrete element modelling. The process in which this will be done is through calculating the energy absorption capacity of a rock type and modelling impacts at different energy levels, then graphing in a similar manner as done in this report.

References

Anglo American Platinum. (2014). *Anglo American Platinum*, 1. Retrieved April 14, 2014, from http://www.angloplat.com

Anglo American Platinum Limited. (2013). *Anglo American Platinum Limited*. Retrieved 10 27, 2014, from http://www.angloplatinum.com/about/about_sub/comp_profile.asp

Asteriou, P., Saroglou, H., & Tsiambaos, G. (2012). Geotechincal and kinematic parameters affecting the coefficients of restitution for rock fall analysis. *International Journal od Rock Mechanics & Mining Sciences*(54), 103-113.

Basson, F. R. (2012). Rigid body dynamics for rock fall trajectory simulation. *46th US Rock Mechanics/Geomechanics* (pp. 1-7). Chicago: American Rock Mechanics Association.

Budetta, P. (2011). Application of the swiss Federal Guidelines on rock fall hazard: a case study in the Cilento region (Southern Italy). *Landslides*(8), 381-389.

California Department of Transportation. (2014). *Division of Engineering Services*. Retrieved 5 14, 2014, from http//www.dot.ca.gov/hq/esc/geotech/geo/edu/page/rm/workshop/pm

Cawthorn, R. G., Walraven, F., Uken, R., & Watkeys, M. K. (2006). The Bushveld Complex. In M. R. Johnson, C. R. Anhaeusser, & R. J. Thomas (Eds.), *The Geology of South Africa* (pp. 261-282). Pretoria: Council for Geoscience.

Chau, K. T., Wong, R. H., & Wu, J. J. (2002). Coefficient of restitution and rotational motions of rockfall impacts. *International Journal of Rock Mechanics & Mining Sciences*(39), 69-77.

Evans, S. G., & Hungr, O. (1989). *books.google.ca*. Retrieved May 5, 2014, from http://books.google.ca/books/about/Geological_Survey_of_Canada_Open_File_20.html?id=ta-o2PB79HQC

Fornaro, M., Peila, D., & Nebbia, M. (1990). Block falls on rock slopes - Applications of a numerical simulation program to some real cases. *International IAEG Congress. 6*, pp. 2173-2180. Rotterdam: Balkema.

Giacomini, A., Buzzi, O., Renard, B., & Giani, G. P. (2009). Experimental studies on fragmentation of rock falls on impact with rock surfaces. *International journal of Rock Mechanics & Mining Sciences*(46), 708-715.

Giacomini, A., Thoeni, K., Lambert, C., Booth, S., & Sloan, S. W. (2012). Experimental study on rockfall drapery systems for open pit highwalls. *International Journal of Rock Mechanics & Mining Sciences*(56), 171-181.

Giancoli, D. (2005). *Physics* (6th ed.). (J. Challice, Ed.) Upper Saddle River, NJ 07458: Pearson Education, Inc.

Giani, G. P., Giacomini, A., Migliazza, M., & Segalini, A. (2004). Experimental and Theoretical Studies to Improve Rock Fall Analysis and Protection Work Design. *Rock Mechanics and Rock Engineering, 5*(37), 369-389.

Goldsmith, W. (2001). *Impact, The theory and physical behaviour of colliding solids.* New York: Dover Publications, Inc.

Guzzetti, F., Crosta, G., Detti, R., & Agliardi, F. (2002). Stone: a computer program for the three-dimensional simulation of rock-falls. *Computers & Geosciences*(28), 1079-1093.

Hoek, E. (2006). *Practical Rock Engineering* (http://www.rocscience.com/hoek/pdf/Practical_Rock_Engineering.pdf ed.). Toronto: Unpublished Notes.

Hoek, E. (2009). Fundamentals of slope design. *Slope Stability*, (pp. 1-16). Santiago.

Hoek, E., & Bray, J. (2005). *Rock Slope Engineering. Civil and Mining.* (4th ed.). (D. C. Wyllie , & C. W. Mah, Eds.) New-York: Spon Press.

Hungr, O., & Evans, S. G. (1993). *The failure behaviour of large rockslides in mountainous regions* (2598 ed.). Vancouver: Geological Survey of Canada .

Imre, B., Rabsamen, S., & Springman, S. M. (2008). A coefficient of restitution of rock materials. *Computers & Geosciences.*(34), 339-350.

Jager, A. J., & Ryder, J. A. (2002). *A textbook on Rock Mechanics for tabular hard rock mines.* (1st ed.). Johannesburg: The Safety in Mines Research Advisory Committee.

Little, M. (2006). *Geotechnical stratigy and tactics at Anglo Platinum's PPRust open pit operation, Limpopo Province, South Africa.* Johannesburg: University of the Witwatersrand.

Read, J., & Stacey, P. (2008). *Guidelines for open pit slope design.* Collingwood Australia: CSIRO.

Richards, L. (1992). Slope stability and rockfall problems in rock masses. In F. G. Bell (Ed.), *Engineering in Rock Masses* (pp. 209-230). Butterworth-Heinemann.

Rocscience. (2003, September 30). *http://www.rocscience.com/assets/files/uploads/8388.pdf*. Retrieved January 12, 2013, from www.rocscience.com

Spadari, M., Giacomini, A., Buzzi, O., Fityus, S., & Giani, G. P. (2012). In situ rockfall testing in New South Wales, Australia. *International Journal of Rock Mechanics & Mining Sciences*(49), 84-93.

Ulusay, R., & Hudson, J. A. (2007). The complete ISRM Suggested Methods for Rock Characterization. In *Testing and Monitoring: 1974-2006* (p. 628p). Commission on Testing Methods, International Society of Rock Mechanics.

Wang, J., Feng, B., Hex, I., Sui, D., Tang, Y., & Yang, P. (2007). *A case study on the impact of rock fall on highway bridge.* Key Laboratory of Geotechnical and Underground Engineering of Ministry of Education, Department of Geotechnical Engineering. Shanghai: Tongli University.

Wang, Y., & Tonon, F. (2011). Discrete Element Modeling of Rock Fragmentation upon Impact in Rock Fall Analysis. *Rock Mechanics Rock Engineering*(44), 23-35.

Wyllie, D. C. (2014). Calibration of rock fall modeling parameters. *International Journal of Rock Mechanics & Mining Sciences*(67), 170-180.

Youssef, A. M., & Maerz, N. H. (2010). Development, justification and verification of a rock fall hazard rating system. *Bulliten of Engineering Geology and the Envitronment*(71), 171-186.